

Metamorphic and structural evolution of the Flin Flon – Athapapuskow Lake area, west-central Manitoba

Manuele Lazzarotto, David R.M. Pattison, Simon Gagné, and Paul G. Starr

Abstract: The Flin Flon – Athapapuskow Lake area, situated in the Flin Flon Greenstone Belt, Manitoba, consists of ocean-floor and island-arc assemblages, deformed and metamorphosed during the Trans-Hudson Orogeny (~1.86–1.69 Ga). A new map of metamorphic mineral assemblages and isograds has been compiled that reveals a largely coherent regional metamorphic sequence increasing in metamorphic grade from prehnite–pumpellyite to amphibolite facies. Regional metamorphism post-dates most of the deformation within the area, with the exception of the reactivation of major block-bounding faults. The regional prograde sequence has been subdivided into 10 metamorphic zones, separated by 9 isograds, that describe the transition from prehnite–pumpellyite to greenschist to amphibolite facies. The formation of contact metamorphic aureoles, pre-dating regional metamorphism, record conditions up to amphibolite facies. Equilibrium phase diagrams for the island-arc (low-Mg) and ocean-floor (high-Mg) assemblages were calculated and allow for the evaluation of the modelling techniques and determination of pressure–temperature conditions. Discrepancies between the modelling predictions and natural observations occur due to (1) limitations in the thermodynamic models for some of the complex minerals (e.g., amphibole); and (2) metastable persistence of some minerals to higher grade due to sluggish reaction kinetics. Notwithstanding these discrepancies, the modelling suggests that metamorphosed mafic rocks in the Flin Flon – Athapapuskow Lake area reached about 430–480 °C and 3.0–4.5 kbar. Peak metamorphic conditions within contact aureoles that preceded regional metamorphism did not exceed 500 °C (at a pressure between 2.7 and 4.4 kbar). The metamorphic field gradient records a transition from 250–300 °C/1.5–2.3 kbar to 430–480 °C/3–4.5 kbar (100–150 °C/kbar), defining a geothermal gradient of approximately 25–31 °C/km.

Key words: metamorphic petrology, greenstone belt, thermodynamic modelling, metamorphic field gradient.

Résumé : Le secteur de Flin Flon – lac Athapapuskow, dans la ceinture de roches vertes de Flin Flon au Manitoba, est constitué d'assemblages du fond océanique et d'arc insulaire, déformés et métamorphosés durant l'orogénèse trans-hudsonienne (~1,86–1,69 Ga). Une nouvelle carte des assemblages minéraux et isogrades métamorphiques a été compilée et révèle une séquence métamorphique régionale généralement cohérente dans laquelle le degré de métamorphisme augmente du faciès à prehnite–pumpellyite à celui à amphibolites. Le métamorphisme régional a succédé à la majeure partie de la déformation dans la région, à l'exception de la réactivation d'importantes failles bordant des blocs. La séquence prograde régionale a été subdivisée en 10 zones métamorphiques séparées par 9 isogrades, qui décrivent la transition du faciès à prehnite–pumpellyite à celui à schistes verts, puis à celui à amphibolites. La formation d'auréoles de contact métamorphiques, qui a précédé le métamorphisme régional, témoigne de conditions allant jusqu'au faciès à amphibolites. Des diagrammes d'équilibre des phases pour les assemblages d'arc insulaire (faibles en Mg) et du fond marin (riches en Mg) ont été obtenus et permettent l'évaluation des techniques de modélisation et la détermination des conditions de pression et température. Des divergences entre les prédictions obtenues par modélisation et les observations se produisent en raison (1) des limites dans les modèles thermodynamiques pour certains minéraux complexes (p. ex. l'amphibole) et (2) la persistance métastable de certains minéraux à des degrés de métamorphisme élevés causée par une cinétique de réaction lente. En dépit de ces divergences, la modélisation donne à penser que des roches mafiques métamorphosées dans le secteur de Flin Flon – lac Athapapuskow ont atteint des températures d'environ 430–480 °C et des pressions de 3,0–4,5 kbar. Les conditions du pic du métamorphisme dans les auréoles de contact formées avant le métamorphisme régional n'ont pas dépassé 500 °C (à une pression entre 2,7 kbar et 4,4 kbar). Le gradient métamorphique de terrain reflète une progression de 250–300 °C/1,5–2,3 kbar à 430–480 °C/3–4,5 kbar (100–150 °C/kbar), ce qui définit un gradient géothermique d'environ 25–31 °C/km. [Traduit par la Rédaction]

Mots-clés : pétrologie métamorphique, ceinture de roches vertes, modélisation thermodynamique, gradient métamorphique de terrain.

Introduction

The Flin Flon greenstone belt (FFB) is situated in west-central Manitoba and east-central Saskatchewan, Canada. It is 240 km wide and extends for about 40 km from the erosional edge of the

Paleozoic formations of the Western Canada Sedimentary Basin in the south, to the gneisses and schists of the Kiseynew Gneiss Belt (KGB) in the metamorphic core of the Trans-Hudson Orogen, in the north (Fig. 1; Hoffman 1988; Bickford et al 1990). The portion

Received 18 July 2019. Accepted 24 March 2020.

M. Lazzarotto and D.R.M. Pattison. Department of Geoscience, University of Calgary, 2500 University Drive NW, Calgary, AB T2N 1N4, Canada.
S. Gagné.* Ottawa, Ontario, Canada.

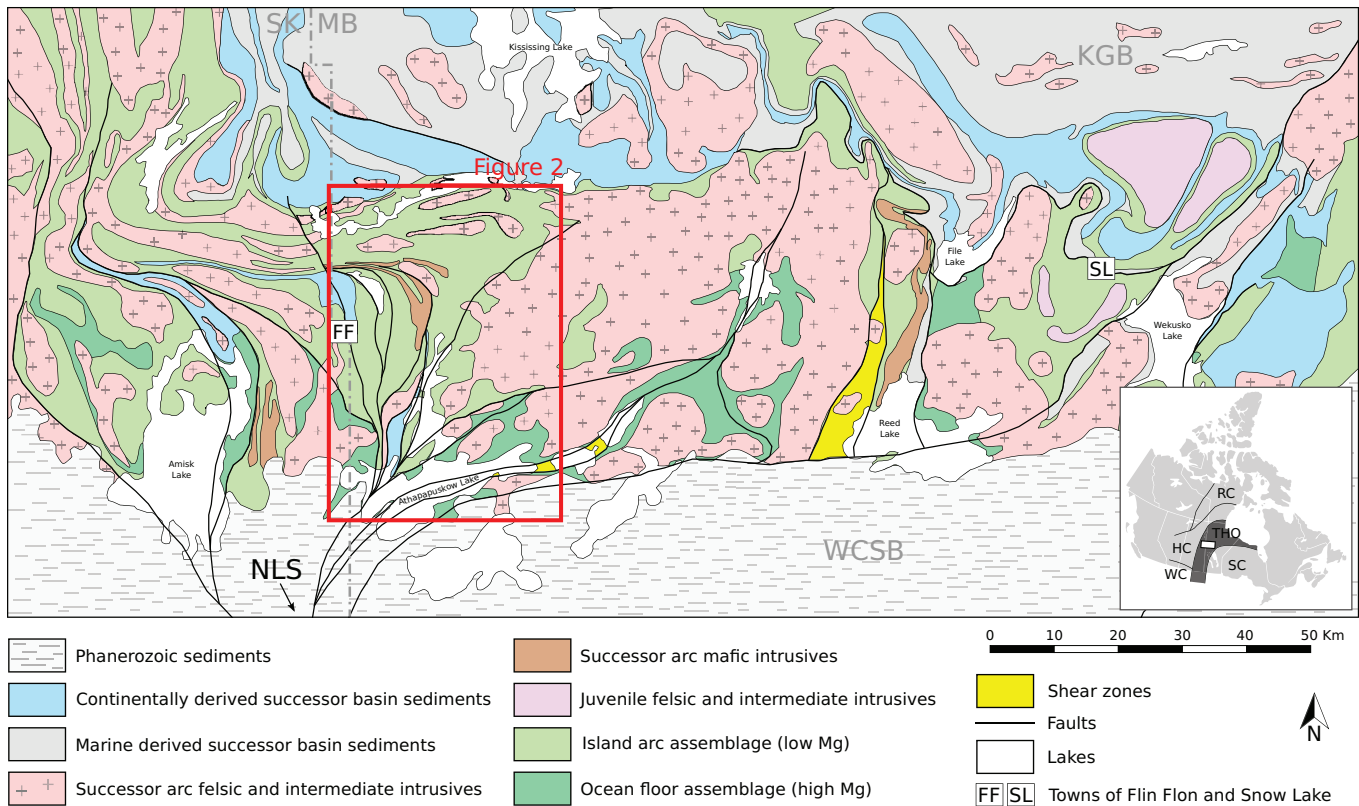
P.G. Starr. Department of Earth and Environmental Sciences, Boston College, 140 Commonwealth Avenue, Chestnut Hill, MA 02467, USA.

Corresponding author: Manuele Lazzarotto (email: manuele.lazzarotto@ucalgary.ca).

*Former address: Manitoba Innovation Energy and Mines, 360-1395 Ellice Avenue, Winnipeg, Manitoba, R3G3P2, Canada.

Copyright remains with the author(s) or their institution(s). Permission for reuse (free in most cases) can be obtained from copyright.com.

Fig. 1. Simplified geology of the Flin Flon greenstone belt (modified from Syme et al. 1998). The box outlined in red shows the study area (Figs. 2a, 2b). KGB, Kisseynew Gneiss Belt; NLS, Nemew Lake Structure; WCSB, Western Canadian Sedimentary Basin. Map created using QGIS version 3.12 (<https://qgis.org/>). [Colour online.]



of the FFB in the Athapapuskow Lake area (Figs. 1, 2) is characterized by an amalgamation of volcanic, intrusive, and sedimentary rocks juxtaposed by a series of shear zones and faults. These units were locally affected by contact metamorphism associated with plutons, and later by regional metamorphism (e.g., Bailes and Syme 1989; Stern et al. 1995a, 1995b; Syme 2015). The Flin Flon – Athapapuskow Lake area (FF-AL) is a prime location to study the metamorphic evolution of the FFB because (1) the area is host to an uninterrupted sequence of metamorphic zones containing units that straddle the transition from prehnite–pumpellyite, through greenschist, to amphibolite facies; (2) several different regional shear zones and faults cut the area, juxtaposing blocks of different origin and metamorphic grade; and (3) relationships between metamorphism in contact aureoles and the later regional metamorphic overprint can be studied around several plutons. The most abundant rocks in the FF-AL are metamorphosed mafic volcanic sequences, which form the main focus of the study, with subordinate felsic metavolcanic and metasedimentary rocks.

As part of this work, a new high-resolution metamorphic map for a 1800 km² area of the FFB is presented that integrates an extensive new sample set augmented by a comprehensive data compilation from the literature. A detailed data set of mineral assemblages, textures, and compositions, combined with lithological and structural information, is used for precise identification of the locations of metamorphic mineral isograds to generate a better understanding of the spatial and genetic relationship between plutonic activity, deformation, and metamorphism. This data set is complemented by thermodynamic phase equilibria modelling and analysis of the sensitivity of the phase equilibria to key modelling inputs. Using this petrological and modelling data set, this work aims to (1) refine the understanding of the metamorphic evolution of the FF-AL, in particular focusing on the relationship between the contact and regional metamorphism and the

plutonic and deformation history; (2) assess the ability of the thermodynamic modelling techniques to reproduce the observed evolution of mineral assemblages, modes, and compositions in the Flin Flon sequence; (3) estimate pressure–temperature (P–T) conditions for the metamorphism of the FF-AL; and (4) derive a metamorphic field gradient for this portion of the FFB.

Previous work on metamorphism and deformation

Heywood (1966) was the first to recognize zones of amphibolite-facies mineral assemblages around granitoid plutons (contact metamorphism) and regional metamorphic prehnite–pumpellyite facies mineral assemblages in the western FFB. Digel and Ghent (1994) and Digel and Gordon (1993) mapped the first appearance of prehnite and pumpellyite in the Schist Lake area, in the southwestern part of the FF-AL. Around the town of Flin Flon within the western part of the study area, metamorphism has been investigated by Starr and Pattison (2019a, 2019b) and Starr et al. (2020). These authors reported conditions of 1.5–2.3 kbar and 250–300 °C for the prehnite–pumpellyite–greenschist facies transition and 3.3–4.4 kbar and 450–500 °C for greenschist–amphibolite facies transition. Prehnite–pumpellyite to upper greenschist facies assemblages were mapped by Bailes and Syme (1989) in the White Lake area, east of Flin Flon. Syme (2015) identified regional and contact metamorphic patterns in the Athapapuskow Lake and Schist Lake areas. The greenschist to amphibolite facies transition from the FFB into the KGB at Kisseynew Lake, has been studied by Jungwirth et al. (2000) and Gilbert (2012), who reported metamorphic peak conditions of 2.3–3.6 kbar and 500–560 °C at the edge of the gneiss belt. In the amphibolite-facies rocks of the Snow Lake and File Lake areas, Kraus and Menard (1997) and Bailes and McRitchie (1978) reported conditions of about 4–6 kbar and 500–700 °C.

Structures in the western part of the FFB were investigated by Bailes and Syme (1989) and Syme (2015), who recognized that the western part of the FFB is characterized by a collage of fault-bounded blocks. Early studies suggested one main deformation event pre-dating the deposition of the sedimentary units, followed by at least two late deformation events that affected all the units (e.g., Stockwell 1946; Gale et al. 1999). A more recent study by Lafrance et al. (2016) suggested two deformation events prior to the deposition of the Missi Group sediments, followed by two thrusting events.

Regional geology

The FF-AL is situated in the western FFB and is part of the juvenile Reindeer Zone of the Trans-Hudson Orogen, formed from the convergence between the Hearne, Superior and Sask cratons (Hoffman 1988; Ansdell 2005). Circa 1.92–1.88 Ga juvenile-arc (low-Mg) and ocean-floor (high-Mg) rocks were juxtaposed in an accretionary collage as a consequence of arc–arc collision at about 1.88–1.87 Ga (Lucas et al. 1996). Post-accretion and successor-arc magmatism (e.g., Whalen et al. 1999) resulted in the emplacement of calcalkalic plutons ca. 1.87–1.83 Ga (Lucas et al. 1996). Between 1.85 and 1.84 Ga, continental and marine sediments were deposited (Missi and Burntwood groups, Ansdell et al. 1995; Lucas et al. 1996). Collisions with the Sask craton at 1.84–1.83 Ga and with the Superior craton at 1.83–1.80 Ga (Bleeker 1990; Ellis et al. 1999; Ashton et al. 2005) resulted in the imbrication and deformation of volcanics and sedimentary rocks along structures active during the early stages of the evolution of the FFB (Lucas et al. 1996; Stern et al. 1999).

The FF-AL consists of imbricated juvenile-arc, ocean-floor, and sedimentary rocks, separated by shear zones and faults, and intruded by plutons, (Figs. 1, 2; Bailes and Syme 1989; Stern et al. 1995a; Lucas et al. 1996). The arc-related assemblages comprise a wide range of volcanic, volcanoclastic, and related synvolcanic intrusive rocks, whereas the ocean-floor assemblages are mainly composed of mid-ocean-ridge basalt and related mafic–ultramafic complexes (Syme and Bailes 1993; Stern et al. 1995b; Lucas et al. 1996). Sedimentary rocks principally consist of thick sequences of continentally derived conglomerate and sandstone, and marine turbidites (Stern et al. 1999; Syme et al. 1999). Fedorowich et al. (1995) and Schneider et al. (2007) defined three main episodes of metamorphism in the FFB: (1) early contact metamorphism around plutons emplaced after the main accretionary stage at ca. 1.86–1.84 Ga; (2) regional subgreenschist- to amphibolite-facies metamorphism ca. 1.82–1.79 Ga; and (3) retrograde overprint at 1.79–1.69 Ga.

The KGB principally consists of migmatitic marine-derived paragneisses (comparable with Burntwood Group in the FFB) and migmatitic continentally derived paragneisses (comparable with Missi Group in the FFB). It has been argued that the KGB and the FFB were juxtaposed during collision of the Flin Flon – Glennie complex with the Sask and Superior cratons before 1820 Ma (e.g., Moore and Froese 1972; Bailes and McRitchie 1978; Zwanzig and Bailes 2010), and the full lithotectonic stack was subsequently metamorphosed between 1820 and 1750 Ma (Bailes 1980; Jungwirth et al. 2000). Kraus and Menard (1997) and Bailes and McRitchie (1978) estimated metamorphic peak conditions of 600–750 °C and 5–6 kbar for the central part of the KGB. The boundary between the FFB and the KGB is marked by a steep metamorphic gradient, which increases from greenschist to upper-amphibolite facies, locally the site of a fault with sinistral sense of shear (Ashton 1993; Zwanzig and Bailes 2010; Gilbert 2012).

Overview of structural features and evolution

Previous studies have shown that the FF-AL experienced a complex multiphase deformation history involving 5–7 deformation events (e.g., Bailes and Syme 1989; Gale et al. 1999; Lafrance et al. 2016). These studies have shown that faults and shear zones in the FF-AL separate distinct blocks of different lithology, and locally of different metamorphic grade (e.g., Bailes and Syme 1989; Syme 2015). In this section, we provide a summary of the major structural features within the FF-AL, focusing on the timing of deformation relative to the regional metamorphism and the major large-scale tectonic events involved in the formation of the Trans-Hudson Orogen. A detailed account of the structural characteristics of individual fault zones is contained within the supplementary information (Supplementary Appendix S3¹) and the locations of the major fault zones within the FF-AL are indicated in Fig. 2a.

The structures in the FF-AL vary from discrete (<1 m wide) brittle faults (e.g., Ross Lake fault) to wide zones of intensely sheared and ductilely deformed rocks (e.g., Northeast Arm shear zone). Some faults and shear zones displace isograds, whereas others are transected by isograds, suggesting reactivation indicative of a prolonged polyphase deformation history. Rocks within these structures comprise greenschist facies assemblages, even in cases where the adjacent units on either side of the shear zone are metamorphosed under prehnite–pumpellyite or amphibolite facies conditions. Faults and shear zones have been categorized based on structural style (e.g., brittle vs. ductile), cross-cutting relationships, and timing with respect to intrusions and metamorphism. Combining previous work with the results of this study, the following interpretations are made:

1. The earliest structures include the north–northeast-trending Northeast Arm, and Mistik Creek shear zones and the Inlet Arm fault, and the west–northwest-trending West Arm shear zone (Fig. 2a). These structures are characterized by ductile fabrics and were active prior to the regional metamorphic event. They juxtapose different lithostratigraphic units and are interpreted to be associated with accretion of the island-arc and ocean-floor assemblages before 1870 Ma. Most of these structures were reactivated during subsequent deformation events.
2. The next generation of north–south-oriented structures, including the Cliff Lake fault, is characterized by ductile deformation that displaces the metamorphic isograds. These structures were active after the deposition of the Missi Group sediments at ca. 1850–1840 Ma as indicated by the truncation of one of its units east and north of the town of Flin Flon (Fig. 2a).
3. Reactivation of early structures after the metamorphic peak is suggested by the displacement of isograds, and by differences in metamorphic grade within the structure compared with the surrounding host rocks. Re-activated structures include the Cliff Lake fault, Northeast Arm and Mistik Creek shear zones, Inlet Arm fault, and possibly the West Arm and South Athapapuskow shear zones. These late movements are interpreted to be the result of continued collision between the accreted arcs and the Sask and Superior cratons after peak metamorphism.
4. The youngest structures include the North Arm, Payuk Lake, and Ross Lake faults. These cut older structures, displace metamorphic isograds, and are characterized by brittle–ductile fabrics. Because these faults were active after the metamorphic peak, they must be younger than 1820–1805 Ma. Movement along these structures is ascribed to late post-collisional tectonism, and possibly tectonic relaxation.

¹Supplementary data are available with the article through the journal Web site at <http://nrcresearchpress.com/doi/suppl/10.1139/cjes-2019-0136>.

Fig. 2. (a) Simplified geology of the Flin Flon – Athapapuskow Lake area with sample locations (black dots) and known mineral deposits (yellow stars); (b) map of regional metamorphic mineral assemblages, isograds, and metamorphic zones of the Flin Flon – Athapapuskow Lake area. Contact metamorphic areas are shown separately in Fig. 6. Data compiled from Bailes and Syme (1989), Gilbert (2012), Syme (2015), Starr (2017), Starr and Pattison (2019a, 2019b), Starr et al. (2020), and samples collected by the authors. Abbreviations (mineral abbreviations after Whitney and Evans 2010): Ab, albite; Act, actinolite; Amp, amphibole; Bt, biotite; Chl, chlorite; Ep, epidote; Grt, garnet; Hbl, hornblende; Olg, oligoclase; Pl, plagioclase; Prh, prehnite; Pmp, pumpellyite; Qtz, quartz; CLF, Cliff Lake fault; IAF, Inlet Arm fault; MCSZ, Mistik Creek shear zone; NAF, North Arm fault; NEASZ, Northeast Arm shear zone; PLF, Payuk Lake fault; RLF, Ross Lake fault; SASZ, South Athapapuskow shear zone; WASZ, West Arm shear zone; EPC, East plutonic complex; KLP, Kaminis Lake pluton; LLP, Lynx Lake pluton; MLA, Mystic Lake assemblages; MLS, Mikanagan Lake sill; MNP, Mink Narrows pluton; NLP, Neso Lake pluton; CP, Cranberry Portage; FF, Flin Flon. Maps were created using QGIS version 3.12 (<https://qgis.org/>). [Colour online.]

Pre-metamorphic igneous rocks

This section contains a summary of the main characteristics of pre-metamorphic volcanic and intrusive rocks. The latter are responsible for contact metamorphism in the FF-AL.

Influence of igneous textures and other remnants on metamorphic assemblages

At outcrop scale, igneous structures are preserved in the form of pillows and flows (Fig. 3a). In most cases, pillow basalts display bulk compositional zonation with pillow cores enriched in CaO and SiO₂, whereas pillow rims contain higher MgO and FeO (Starr and Pattison 2019a; Starr et al. 2020; this work). This compositional zonation is manifested as mineralogical zonation within the later metamorphic assemblages. Typically, at greenschist and amphibolite facies conditions, pillow cores are rich in epidote and contain small amygdaloids, whereas the rims contain more chlorite and actinolite/hornblende, with more and larger amygdaloids. Within shear zones, pillows are elongate commonly showing stronger deformation in selvages compared with the pillow cores. Original plagioclase and (or) clinopyroxene phenocrysts, now pseudomorphed by metamorphic minerals, are typically aligned, preserving the trachytic texture commonly observed in magmatic flows. Preservation of such igneous fabrics is commonly observed in samples from the subgreenschist and greenschist facies, but primary structures are mostly overprinted within amphibolite facies samples. With the exception of samples within shear zones that experienced post-metamorphic deformation, the metamorphic mineralogy is randomly oriented and controlled texturally by relict igneous features such as phenocrysts and amygdaloids.

Preservation of igneous mineralogy is rare. Only a few samples within the subgreenschist facies contain relict igneous pyroxene. Generally, pyroxene is replaced by actinolite and (or) hornblende and chlorite, depending on metamorphic grade. Igneous calcic plagioclase is not preserved and is replaced, at subgreenschist facies, by albite (with minor prehnite, pumpellyite, and epidote), and by oligoclase (with minor albite, epidote, and carbonate) at the greenschist–amphibolite transition and amphibolite facies conditions.

Overview of intrusive rocks

The FF-AL area is characterized by a large number of plutonic bodies that vary in age from 1884 to 1843 Ma (Whalen et al. 2016). These plutonic bodies can be broadly grouped into those that formed prior to the deposition of the Missi group sediments (Flin Flon arc assemblage or early successor arc), such as the Neso Lake pluton, and those formed after the deposition of the Missi group (late successor arc), such as the Lynx Lake pluton (Fig. 2). All plutonic activity occurred prior to the regional metamorphic event as indicated by the absence of contact metamorphic assemblages that overprint the regional metamorphism. For a more detailed description of individual plutons, the reader is referred to Zwanzig and Bailes (2010), Gilbert (2012), and Syme (2015).

Regional metamorphism

With the exception of the Phanerozoic sedimentary cover south of Athapapuskow Lake, all rocks in the FF-AL experienced regional

metamorphism that post-dated emplacement of the intrusions and the associated contact metamorphism (Fig. 2b). Two major regional metamorphic-facies transitions in metamorphosed mafic rocks are observed: the prehnite–pumpellyite- to greenschist-facies transition and the greenschist- to amphibolite-facies transition.

Metamorphic mineral assemblages, zones, and isograds

Figure 2b shows a map of metamorphic-mineral assemblages and isograds of the Athapapuskow Lake area. The map was created using samples collected by the authors, in addition to data from Bailes and Syme (1989), Gilbert (2012), Syme (2015), Starr (2017), Starr and Pattison (2019a, 2019b), and Starr et al. (2020). The plotted mineral assemblages comprise key mineral associations used to define the metamorphic zones and the full mineral assemblages are recorded in Supplementary Appendix S1¹. The metamorphic zones, ranging from prehnite–pumpellyite to amphibolite facies, are defined by specific combinations of the minerals prehnite, pumpellyite, actinolite, biotite, hornblende, albite, oligoclase, chlorite, epidote, and garnet.

A northerly increase in metamorphic grade is observed, as part of a single, relatively coherent metamorphic sequence, from prehnite–pumpellyite facies in the southern part of Schist Lake to garnet–amphibolite facies at the contact with the KGB. From south to north, nine isograds were defined: actinolite-in, prehnite- and pumpellyite-out, biotite-in, hornblende-in, oligoclase-in, actinolite-out, epidote-out, chlorite-out, and garnet-in. An exception is the cryptic amphibolite-facies domain, referred to as the “Mystic Lake assemblage” (Fig. 2a; see “Mystic Lake assemblage” section below), outcropping in the southwestern part of the study area. Below, the metamorphic zones and isograds are described in sequence from low to high grade.

Prehnite–pumpellyite facies

Prehnite–pumpellyite zone

The prehnite–pumpellyite zone is defined as the area down-grade of the actinolite-in isograd and is characterized by the mineral assemblage Prh+Pmp+Ab+Chl+Ep+Qtz±Ttn±Cb±Ms±Ap (Fig. 4a) (abbreviations after Whitney and Evans 2010). It extends for up to 12 km north of the Paleozoic unconformity (Fig. 2b). Typically, prehnite and pumpellyite coexist within samples of this zone, although prehnite is generally present in higher modal amounts than pumpellyite. Albite, chlorite, epidote, and sericite replace phenocrysts or occur as part of the matrix assemblage. Radial or granular epidote, fibrous chlorite, and quartz also fill amygdaloids.

Prehnite–pumpellyite to greenschist facies transition

Actinolite–prehnite–pumpellyite zone

The actinolite–prehnite–pumpellyite zone is defined as the area between the actinolite-in and prehnite- and pumpellyite-out isograds. The key metamorphic mineral assemblage within this zone is Act+Prh+Pmp+Ab+Chl+Ep+Qtz±Ttn±Cb±Ms±Ap (Fig. 4b), including the coexistence of actinolite with either or both of prehnite and pumpellyite. The zone is 3 km wide in the western part of the study area, and it reaches 9 km wide in the eastern part (Fig. 2b).

Fig. 2 (continued).

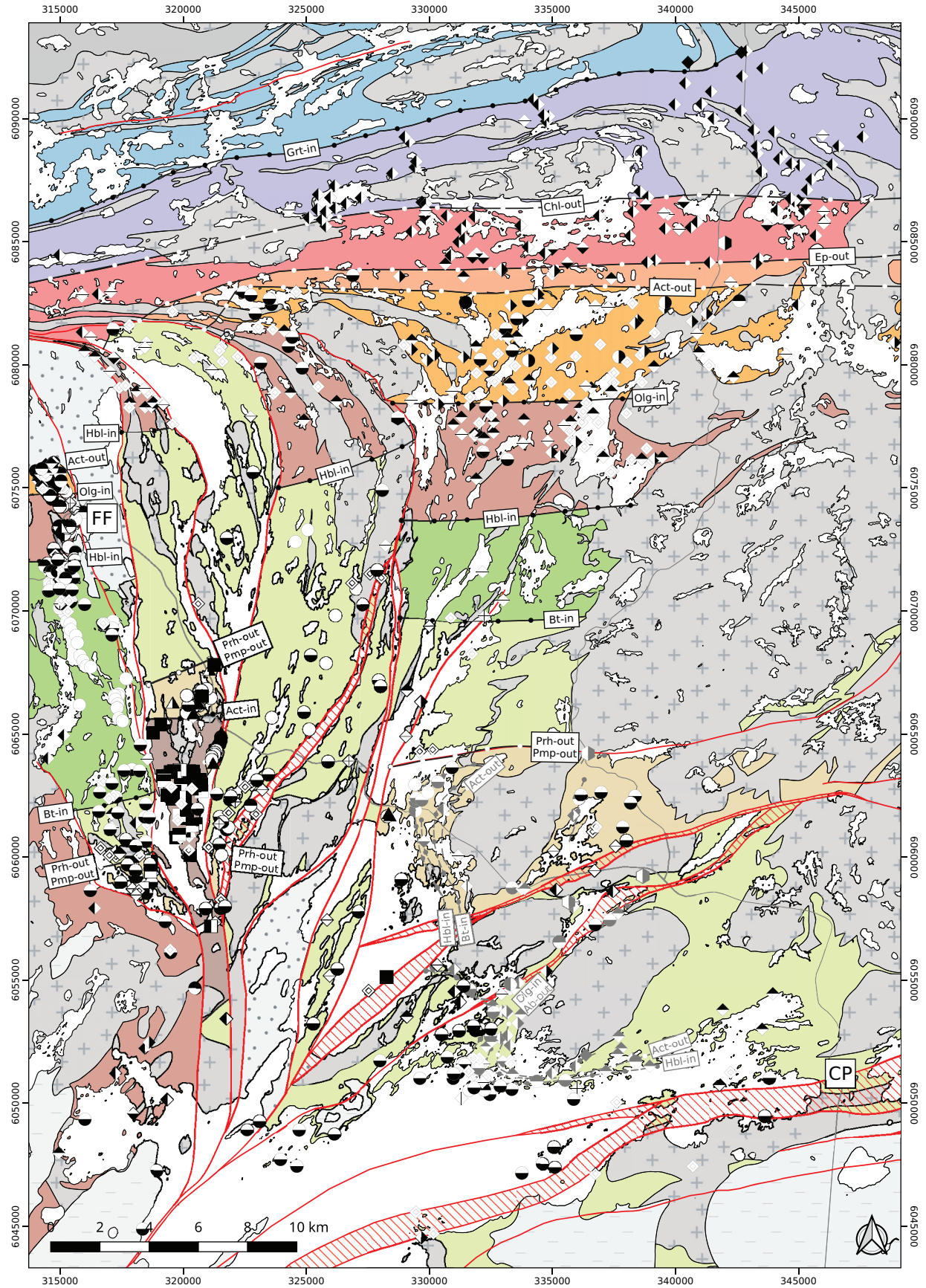


Fig. 4. Photomicrographs of rocks from different metamorphic zones in the study area: (a) prehnite, epidote, and chlorite in amygdule of sample from the prehnite–pumpellyite zone, (plane polarized light (ppl); sample 52-85-342-1); (b) prehnite-filled amygdule in contact with actinolite in sample from the actinolite–prehnite zone (ppl; sample 71-1); (c) actinolite, epidote, and albite in sample from the actinolite–albite zone (ppl; sample 52-88-3010-1); (d) distinct crystals of hornblende and actinolite in sample from the hornblende–actinolite–albite zone (ppl; sample 52-86-1010-1); (e) hornblende, actinolite, and oligoclase in sample from the hornblende–actinolite–oligoclase zone (ppl; sample 52-82-2192-1); (f) hornblende and oligoclase in matrix of sample from the hornblende–oligoclase zone (ppl; sample 32-01-0362-1); (g) hornblende and oligoclase in matrix of sample from the chlorite-free zone (ppl; sample 32-01[hypen-0198-1]); (h) hornblende and garnet in sample from the hornblende–garnet zone (ppl; sample 32-03-0062-1). [Colour online.]

metamorphic-mineral assemblage is $\text{Hbl}+\text{Act}+\text{Olg}+\text{Ab}+\text{Ep}+\text{Chl}+\text{Qtz}\pm\text{Ilm}\pm\text{Ttn}\pm\text{Bt}\pm\text{Ap}\pm\text{Opq}$ (Fig. 4e). This zone differs from the hornblende–actinolite–albite zone in that it contains oligoclase as part of the assemblage, which occurs as a fine-grained interstitial phase to amphiboles. Where albite and oligoclase coexist, they are found both as adjacent individual crystals, and in patchy intergrowths and core-rim microstructures, in which an oligoclase-rich rim mantles an albite-rich core (Figs. 5a, 5b), similar to the observations reported by Starr and Pattison (2019a). The modal amount of hornblende increases with increasing grade at the expense of actinolite, chlorite, and epidote.

Epidote–amphibolite facies

Hornblende–oligoclase–epidote zone

Between the actinolite-out and the epidote-out isograds, the hornblende–oligoclase–epidote zone is found. This zone differs from the hornblende–actinolite–oligoclase zone in that it lacks actinolite and is characterized by the assemblage $\text{Hbl}+\text{Olg}+\text{Ep}+\text{Chl}+\text{Qtz}\pm\text{Bt}\pm\text{Ilm}\pm\text{Ttn}\pm\text{Ap}\pm\text{Opq}$ (Fig. 4f). The zone is typically less than 1 km wide (Fig. 2b). Epidote is fine grained and granular and decreases in modal amount towards the epidote-out isograd.

Amphibolite facies

Hornblende–oligoclase zone

The zone between the epidote-out and chlorite-out isograd is defined as the hornblende–oligoclase zone and has the characteristic mineral assemblage $\text{Hbl}+\text{Olg}+\text{Chl}+\text{Qtz}\pm\text{Bt}\pm\text{Ilm}\pm\text{Ttn}\pm\text{Ap}\pm\text{Opq}$. The zone is up to 4 km wide from south to north (Fig. 2b) and differs from the hornblende–oligoclase–epidote zone in that it lacks epidote. A decrease in the modal amount of chlorite towards the north is observed in this zone.

Chlorite-free zone

The zone north of the chlorite-out and south of the garnet-in isograd is defined as the chlorite-free zone. This zone extends for up to 5 km (Fig. 2b), and is characterized by the absence of chlorite, with the key mineral assemblage $\text{Hbl}+\text{Olg}+\text{Qtz}\pm\text{Bt}\pm\text{Ilm}\pm\text{Ttn}\pm\text{Ap}\pm\text{Opq}$ (Fig. 4g). Fine-grained oligoclase, interstitial to aggregates or blades of dark green hornblende, and platy brown biotite, make up the majority of the rock. Ilmenite and Fe-sulfides are the main opaque minerals.

Hornblende–garnet zone

The hornblende–garnet zone represents the highest metamorphic grade found in the FFB. The zone extends up to 6 km from south to north (Fig. 2b) and is bound to the south by the garnet-in isograd and to the north by the high grade migmatitic metasedimentary rocks of the KGB. The metabasite metamorphic sequence abruptly ends in the hornblende–garnet zone at the contact with the metasediments of the KGB. The characteristic mineral assemblage for this zone is $\text{Hbl}+\text{Olg}+\text{Bt}+\text{Grt}+\text{Qtz}\pm\text{Ilm}\pm\text{Ap}\pm\text{Opq}$ (Fig. 4h). Where present, garnet porphyroblasts up to 3 mm in diameter overgrow amphibole crystals. Green to blue hornblende grains less than a millimetre to several millimetres long create an interlocking texture. Oligoclase and biotite persist throughout the zone.

Mystic Lake assemblage

The Mystic Lake assemblage (MLA; after type locality in Saskatchewan as suggested by Thomas (1991) and Syme (2015)) is a region of amphibolite-facies rocks approximately 5 km by 5 km in size that occurs southeast of the Kaminitis Lake pluton. It is bound to the east by the Ross Lake fault and the West Arm shear zone, to the north and west by the Kaminitis Lake pluton, and to the south it is unconformably overlain by Paleozoic strata. Rocks in the MLA consist of strongly foliated, fine-grained amphibolite, whose protoliths are basalt, diabase, and mafic tuff. These rocks are inter-layered with deformed, fine-grained felsic layers that appear to represent injections of tonalite, granodiorite, and granite into the mafic host rocks (Fig. 3b). The tonalitic and granitic layers vary between a few millimetres and several centimetres in thickness, and consist of fine-grained quartz and feldspar, with minor muscovite and biotite. The characteristic mineral assemblage for metabasite rocks of this area is $\text{Hbl}+\text{Pl}+\text{Bt}+\text{Chl}+\text{Qtz}\pm\text{Opq}\pm\text{Ap}$. The amphibolite facies assemblage of these rocks is notably higher than the adjacent subgreenschist facies rocks of the Flin Flon arc assemblage, from which it is separated by the West Arm shear zone (Fig. 2b).

Stern et al. (1993) reported a U–Pb age of 1903 \pm 6/–4 Ma for the tonalitic rocks, interpreted as the age of injection. This age of the intrusive rocks in the MLA, and the high degree of deformation of the host rocks, suggests that the MLA is older than the island-arc derived assemblages (1894–1882 Ma; Syme 2015), and younger than the ocean-floor assemblages (1901–1904 Ma; Syme 2015). Lucas et al. (1996) interpreted the MLA as a microcontinental fragment that was emplaced in an early stage of the evolution of the FFB.

Contact metamorphism

Contact metamorphic aureoles around plutons are recognized in the field in areas where the later overprinting regional metamorphism did not exceed greenschist-facies conditions (e.g., Lynx Lake pluton, Mink Narrows pluton, Fig. 2b). The aureoles are most readily identifiable through a general darkening of the fresh and weathered surfaces, which in thin section corresponds to the presence of fine-grained hornblende. Upgrade of the regional hornblende-in isograd, it is difficult to identify contact aureoles because the contact and regional metamorphic rocks contain the same diagnostic mineral assemblages. In the FF-AL, contact aureoles between 1 and 2 km wide have been mapped (Fig. 6) and generally show little evidence for deformation, with preservation of igneous features such as phenocrysts and pillow or flow structures.

A well-developed contact metamorphic aureole up to 1.8 km wide surrounds the Lynx Lake pluton (Fig. 6a) within the regional greenschist facies actinolite–albite zone. Contact metamorphic isograds for hornblende-in, oligoclase-in and albite-out, and actinolite-out were identified, spanning greenschist to lower amphibolite facies conditions. The Lynx Lake pluton contact aureole is characterized by (1) an increase in grain size towards the intrusion; (2) progressive changes from the regional Act–Ab-bearing assemblages, outside the contact aureole, to $\text{Hbl}+\text{Act}+\text{Ab}$, $\text{Hbl}+\text{Act}+\text{Olg}$, and $\text{Hbl}+\text{Olg}$ with increasing proximity to the pluton; and (3) increase in modal amount of hornblende and decrease in the

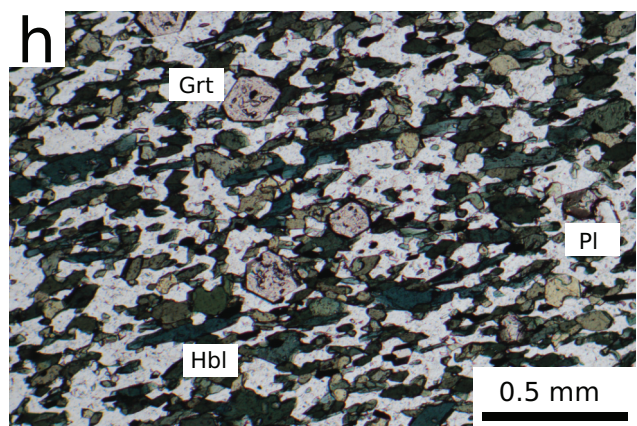
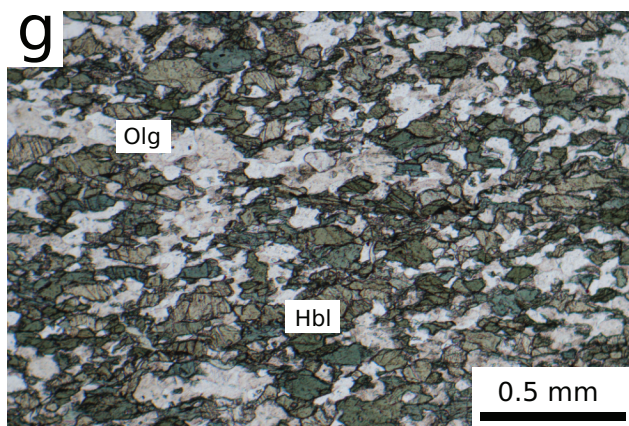
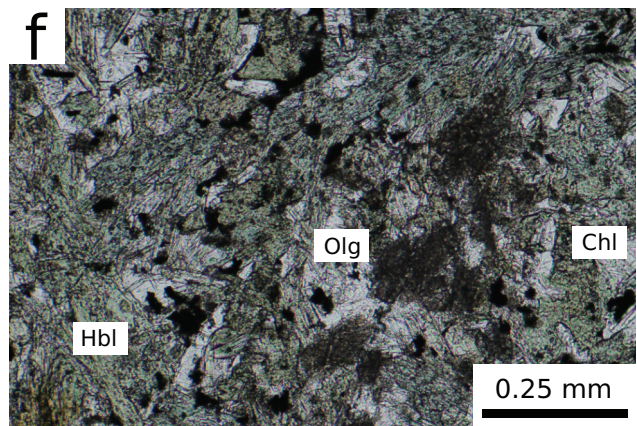
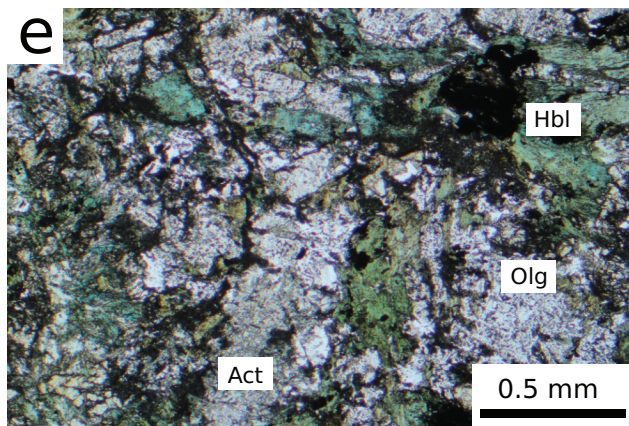
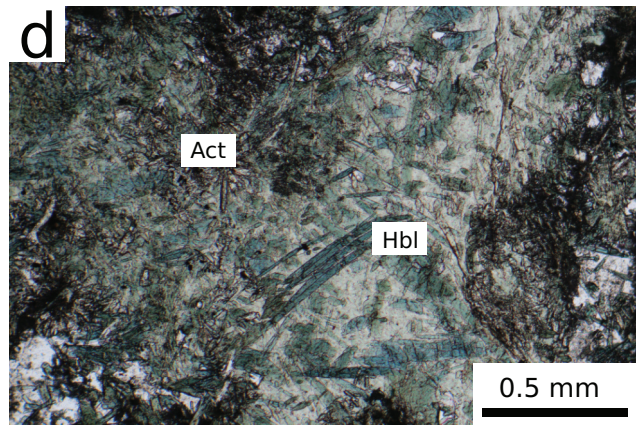
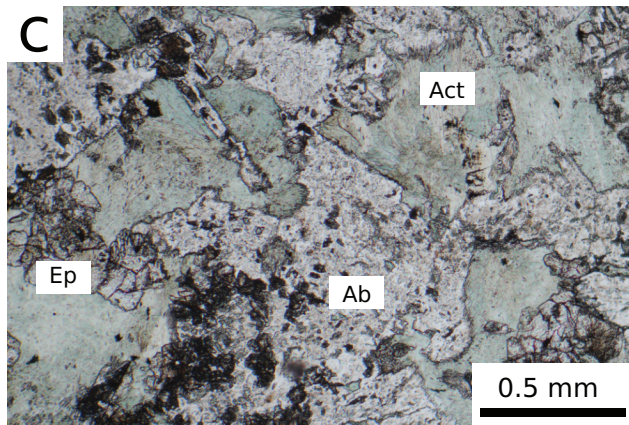
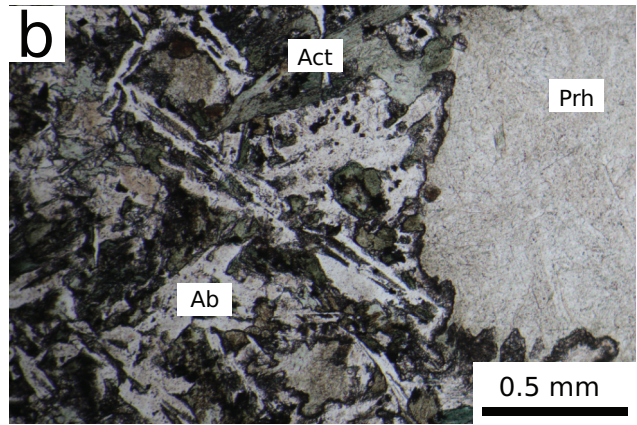
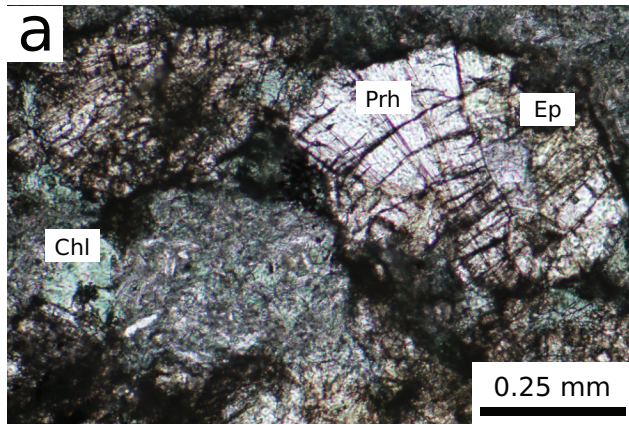
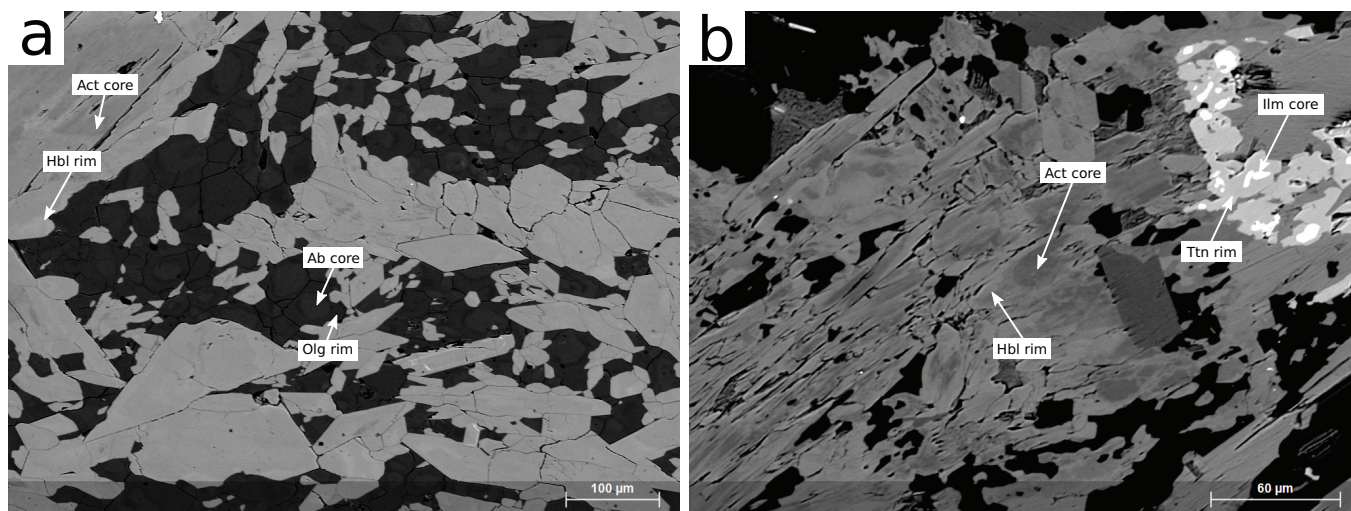


Fig. 5. Back-scattered electrons images. (a) Amphibole zoning (actinolite core and hornblende rim), and feldspar zoning (albite core and oligoclase rim) in sample from the hornblende–actinolite–oligoclase zone (sample 141-1); (b) amphibole zoning (actinolite core and hornblende rim), and ilmenite crystals rimmed by titanite from the hornblende–actinolite–oligoclase zone (sample 147-1).



modal amount of epidote toward the intrusion. Garnet porphyroblasts were found in a single locality in the internal part of the contact aureole and, from their development in transecting domains within a rhyolite host rock (?), likely developed altered bulk compositions.

Around the Neso Lake pluton, a contact aureole up to 2 km wide is observed (Fig. 6b) within the regional subgreenschist facies zone. Contact metamorphic isograds for hornblende-in, oligoclase-in, biotite-in, and actinolite-out were identified. The typical mineral assemblage in the outer part of the aureole is Hbl+Act+Olg+Ep+Chl+Qtz±Ilm±Ttn±Opq, whereas in the internal part the highest grade assemblage Hbl+Olg+Bt+Ep+Chl+Qtz±Ilm±Ttn±Opq is found. Garnet grains were identified at one locality in the highest grade part of the aureole.

A contact aureole extends for approximately 1 km around the Kaminis Lake pluton in the southwestern part of the FF-AL within the regional lower amphibolite facies hornblende–actinolite–albite zone. A metamorphic-mineral assemblage consisting of Hbl+Act+Pl+Bt+Chl+Qtz±Opq±Ap is commonly observed in the aureole. This assemblage differs from the regional assemblage, in that it does not contain albite and generally has a coarser grain size. No contact aureole was distinguished on the southeastern side of the Kaminis Lake pluton, due to the limited samples collected.

Compositions of metamorphic minerals

Quantitative compositional data were obtained by wavelength dispersive spectrometry on a JEOL JXA-8200 electron probe micro analyzer at the University of Calgary, using an acceleration voltage of 15 kV, a current of 20 nA, and a range of well-characterized natural and synthetic standards. Amphibole, plagioclase, chlorite, and epidote were analyzed in a number of representative samples for each metamorphic zone and the data are presented in Supplementary Appendix S2¹. The ferric iron content and site cations for amphibole were calculated using the methods outlined in Schumacher (1997).

Amphibole

Amphiboles occur in the majority of the metamorphosed mafic volcanic rocks within the greenschist- and amphibolite facies. Within the greenschist–amphibolite transition zone, two amphibole phases coexist as a result of a miscibility gap. These two amphiboles are broadly named “actinolite” (Si > 7.5 cations per

formula unit (cpfu) and “hornblende” (Si < 7.5 cpfu) after Leake et al. (1997). Figures 7a and 7b show amphibole compositional data for the FF-AL as a function of metamorphic grade. Most of the amphiboles downgrade of the hornblende-in isograd, classify as actinolite ($^{\text{T}}\text{Si} = 7.3\text{--}8.0$ cpfu, $X_{\text{Mg}} = \text{Mg}/(\text{Fe}^{2+} + \text{Mg}) = 0.4\text{--}0.8$). Upgrade of the hornblende-in isograd, a progressive change in amphibole composition is observed with increasing grade. Within the hornblende–actinolite–albite zone, hornblende classifies as magnesio-hornblende ($^{\text{T}}\text{Si} = 7.0\text{--}7.5$ cpfu, $X_{\text{Mg}} = 0.5\text{--}0.8$), whereas in the hornblende–actinolite–oligoclase zone the hornblende composition is ferro-hornblende ($^{\text{T}}\text{Si} = 6.5\text{--}7.0$ cpfu, $X_{\text{Mg}} = 0.3\text{--}0.5$). No closure of the compositional gap with increasing grade is observed, similar to observations by Starr and Pattison (2019a). Upgrade of the actinolite-out isograd, the amphiboles consist of magnesio- and ferro-hornblende, and minor tschermakite and ferro-tschermakite ($^{\text{T}}\text{Si} = 6.0\text{--}6.7$ cpfu, $X_{\text{Mg}} = 0.3\text{--}0.7$).

Plagioclase

Plagioclase is present in most of the metamorphosed mafic volcanic rocks throughout the study area. In samples from the prehnite–pumpellyite facies, plagioclase is a minor phase, accounting for <10% of the modal amount, whereas it constitutes up to 50% abundance in rocks from the greenschist- and amphibolite-facies. Figure 7c shows the compositional changes of regionally metamorphosed plagioclase with grade. For samples of subgreenschist and lower-greenschist-facies grade, the large majority of the plagioclase is of albitic composition (An₁–An₇). Albite is present together with oligoclase (An₁₅–An₂₇) in rocks of the greenschist–amphibolite transition, upgrade of the oligoclase-in isograd, defining a compositional gap (peristerite gap; e.g., Carpenter 1981; Maruyama et al. 1982; Ashworth and Evirgen 1985; Starr and Pattison 2019a). Upgrade of the actinolite-out isograd, oligoclase comprises up to 70% of the total plagioclase. In some amphibolite-facies assemblages within contact aureoles, usually close to the contact with the intrusion, the anorthite component is as high as An₄₀ (andesine).

Chlorite

Chlorite is present in nearly all samples from the FF-AL, except north of the chlorite-out isograd in the northernmost metamorphic zones, and occurs as both a primary and secondary (retrograde) phase. Primary chlorite is identified as small grains intergrown with other minerals in the matrix, whereas secondary

Fig. 6. Map of the metamorphic-mineral assemblages and isograds (a) for the Lynx Lake pluton contact aureole; (b) for the Neso Lake pluton contact aureole. Legend is the same as Fig. 2. Maps created using QGIS version 3.12 (<https://qgis.org/>). [Colour online.]

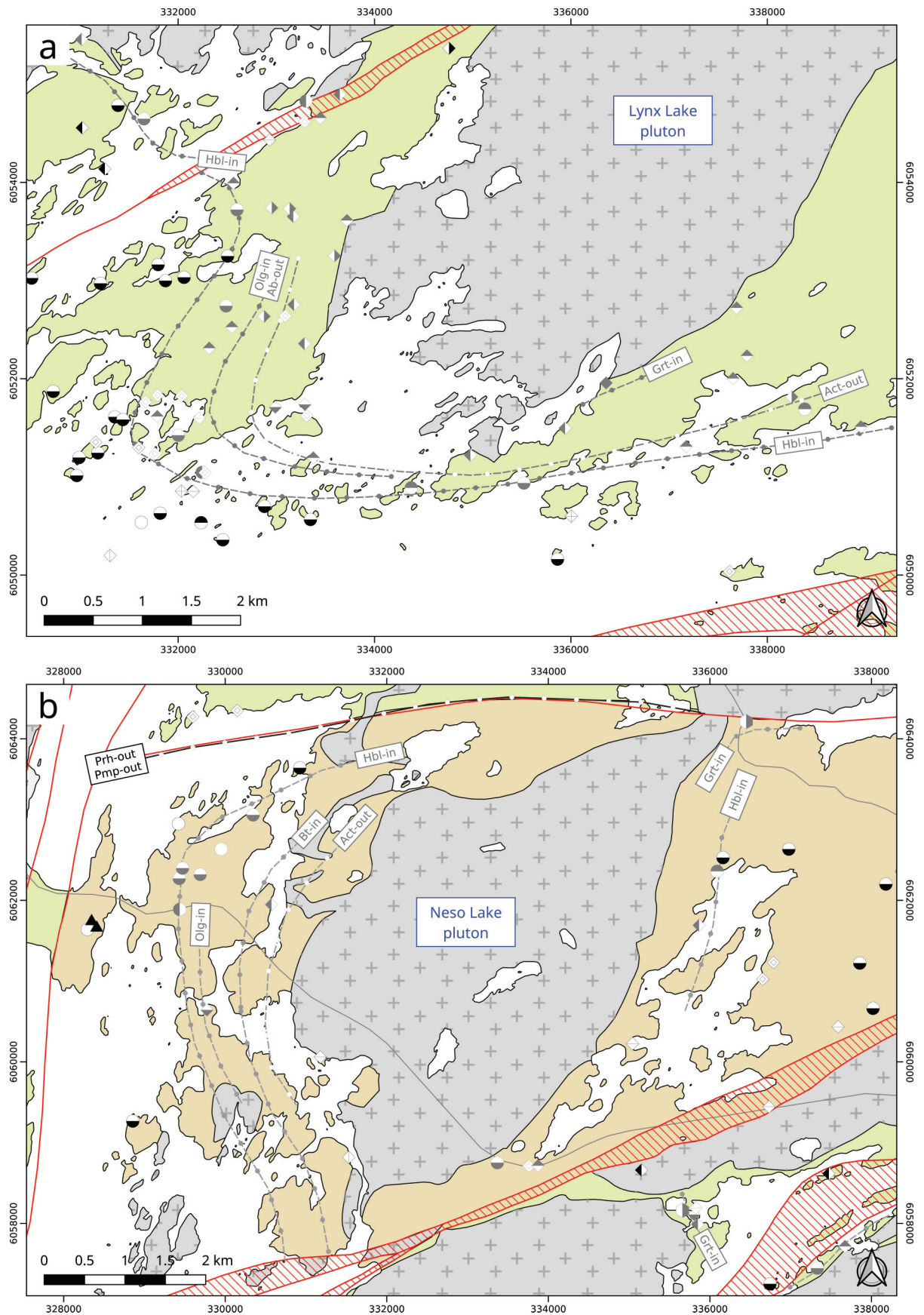
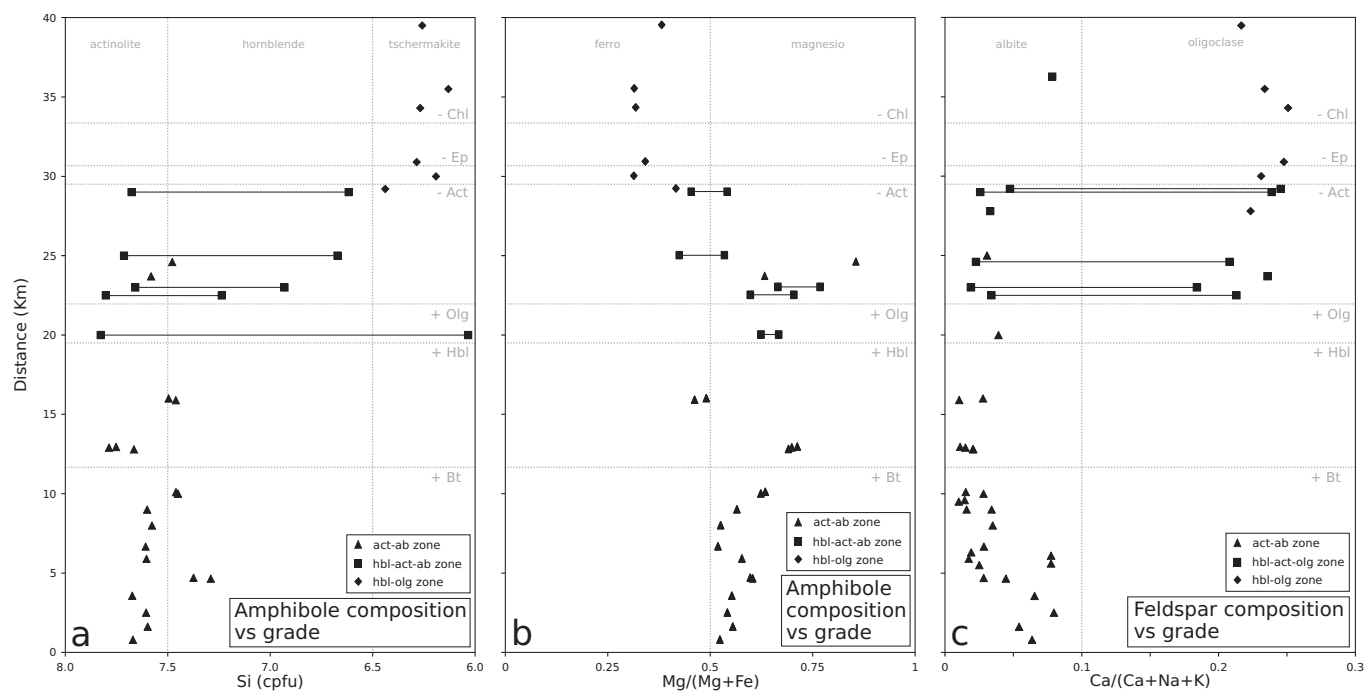


Fig. 7. Mineral chemistry data. (a) Compositions of amphibole (Si cations per formula unit (cpfu)) plotted versus grade; (b) compositions of amphibole (Mg/(Mg+Fe)) plotted versus grade; (c) compositions of feldspars (An content) plotted versus grade.



chlorite is usually found as fracture-filling grains or as blades overgrowing the matrix crystals. Primary chlorite generally decreases in X_{Fe} (defined as $\text{Fe}^{2+}/(\text{Fe}^{2+} + \text{Mg})$) from $X_{\text{Fe}} = 0.50$ in the subgreenschist facies, to $X_{\text{Fe}} = 0.25$ in the amphibolite facies. According to the classification scheme of Hey (1954), chlorite in rocks of the greenschist facies classify as ripidolite/pycnochlorite, and transition to clinocllore in samples of the amphibolite facies (Fig. 8).

Epidote

Epidote is found throughout the mafic volcanic rocks in the subgreenschist- and greenschist-facies although it is less common in higher grade rocks of the greenschist–amphibolite facies transition and amphibolite facies. Primary epidote is present as euhedral crystals or granular aggregates of crystals, whereas secondary epidote is very fine grained and commonly associated with sericite as a breakdown product of plagioclase. Zoning is mostly expressed as gradational zoning between core and rim of crystals, but sharp core-rim or irregular zoning patterns are also observed. Most of the epidote cores have $\text{Ps} > 0.22$, whereas rims have $\text{Ps} < 0.24$, with Ps (pistacite) content defined as $\text{Fe}^{3+}/(\text{Fe}^{3+} + \text{Al})$. These values are similar to those of Starr and Pattison (2019a) for the Flin Flon area.

Other minerals

Titanite is the main Ti-bearing phase downgrade of the hornblende-in isograd. In some cases, ilmenite is rimmed by titanite, interpreted as partial reaction of magmatic ilmenite to metamorphic titanite during prograde metamorphism (Fig. 5b). Above the oligoclase-in isograd, ilmenite becomes the dominant Ti-bearing mineral. Most samples contain carbonate phases of both primary and secondary origin although their modal amount never exceeds 1%–2%. Usually, primary calcite and (or) minor dolomite are found as within vesicles or as irregular blebs in the groundmass whereas secondary carbonates mostly fill fractures. Sulfides, such as pyrite and chalcopyrite, typically occur as disseminated grains (up to 1 mm) within the matrix. No discernible pattern in the sulfide mineralogy or modes with increasing grade has been identified, as also observed by Starr and Pattison (2019a).

Thermodynamic modelling

Equilibrium phase diagrams were created for representative average bulk compositions of the island arc (low-Mg; 177 whole-rock XRF analyses) and the ocean-floor (high-Mg; 41 whole-rock XRF analyses) assemblage rocks for the greenschist–amphibolite facies (Table 1, Fig. 9). For this study, we focus on modelling of the greenschist–amphibolite facies transition as this is where the majority of important mineralogical changes occur, whilst containing phases that we have the ability to model.

The phase diagrams in Figs. 9a–9d are coloured according to the key mineral assemblages used to define the metamorphic zones in Fig. 2b: green, Act+Ab; brown, Hbl+Act+Ab; orange, Hbl+Act+Olg; salmon, Hbl+Ep (“Ep-amphibolite”); red, Hbl+Chl (“Chl-amphibolite”); and purple, Hbl+Olg.

Diagrams were calculated using the Gibbs free energy minimization software suite Theriak-Domino (de Capitani and Brown 1987; de Capitani and Petrakakis 2010), in combination with the internally consistent thermodynamic data set of Holland and Powell (1998; updated to version ds5.5) or the data set of Holland and Powell (2011; updated to version ds6.2). Modelling with both data sets was carried out to test the ability of the different data sets to effectively reproduce the natural observations from the Flin Flon sequence. For calculations with data set ds5.5, the following activity-composition models (a-X models) were used: clin amphibole and clinopyroxene (Diener and Powell 2012), garnet and biotite (White et al. 2007), white mica (Coggon and Holland 2002), chlorite, epidote, talc, and olivine (Holland and Powell 1998), orthopyroxene and magnetite-spinel (White et al. 2002), ilmenite–hematite (White et al. 2000), and feldspar (Cbar1 field; Holland and Powell 2003). For calculations with data set ds6.2, the following a-X relations were used: clin amphibole and augite (Green et al. 2016), garnet, biotite, white mica, chlorite, orthopyroxene (White et al. 2014), epidote and olivine (Holland and Powell 2011), magnetite–spinel (White et al. 2002), ilmenite–hematite (White et al. 2000), and feldspar (Cbar1 field; Holland and Powell 2003).

The modelling was performed in the $\text{Na}_2\text{O}-\text{CaO}-\text{K}_2\text{O}-\text{FeO}-\text{MgO}-\text{Al}_2\text{O}_3-\text{SiO}_2-\text{H}_2\text{O}-\text{TiO}_2-\text{Fe}_2\text{O}_3$ (NCKFMASHTO) chemical system. All P

Fig. 8. Chlorite compositional diagram with data, plot, and fields after Hey (1954). Chlorite composition becomes richer in Mg with increasing grade (arrow). cpfu, cations per formula unit.

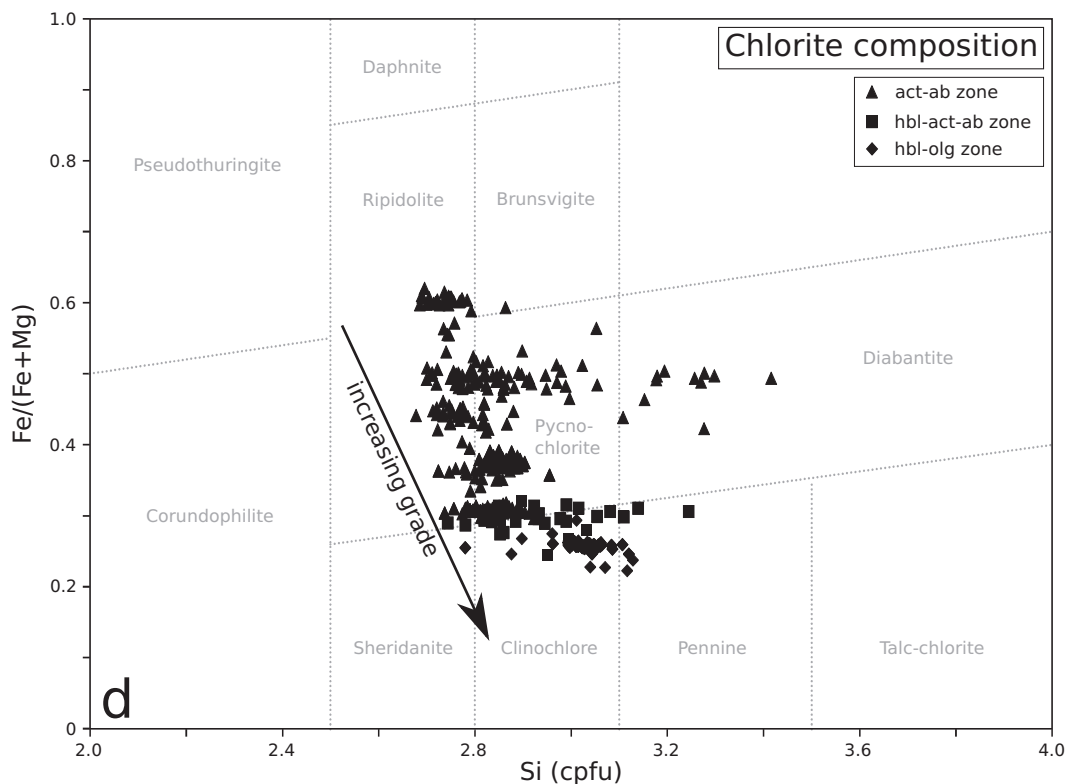


Table 1. Whole-rock geochemical data used to calculate phase-equilibria diagrams of Fig. 9.

	SiO ₂	Al ₂ O ₃	CaO	MgO	FeO	K ₂ O	Na ₂ O	TiO ₂	MnO	P ₂ O ₅	LOI	Total
High-Mg metabasalt	48.923	14.094	8.722	7.147	13.595	0.214	2.513	1.193	0.200	0.137	3.524	100.261
Low-Mg metabasalt	53.837	14.940	7.800	4.980	11.465	0.699	2.692	0.617	0.000	0.126	2.619	99.774

Note: Average calculated based on data from Bailes and Syme (1989), Gilbert (2012), Syme (2015), Starr and Pattison (2019a, 2019b), Starr et al. (2020), and samples collected by the authors. Units are weight % oxides. LOI, loss on ignition.

is assumed to be contained in apatite and H₂O was modelled in excess over the calculated P-T range, appropriate for the subsolidus conditions represented by the range in metamorphic grade in the FF-AL. Ferric iron is an important component in the determination of phase relations of metabasites because of the high modal proportion of Fe³⁺-bearing minerals (e.g., Diener and Powell 2012). The FeO and Fe₂O₃ contents of 10 metamorphosed mafic samples spanning the study area were determined using XRF analysis complemented by ferrous iron titration. The determined XFe³⁺ values ($X_{Fe^{3+}} = Fe_2O_3 / (Fe_2O_3 + FeO)$ in wt%) range from 22% to 31% (equivalent to 11–16 mol% oxides). These values may be affected by post-metamorphic oxidation during weathering and alteration and are therefore interpreted as an upper limit. For both the high-Mg and the low-Mg bulk compositions, P-T sections with different XFe³⁺ of 0%, 10%, 15%, 20%, 30%, and a series of T-XFe³⁺ diagrams with XFe³⁺ between 0% and 30% at 3–5 kbar, were calculated. These diagrams were compared with the natural sequence of mineral assemblages in the FF-AL to determine the XFe³⁺ value that best corresponds to the observed sequence of isograds. The calculations suggest that for both bulk compositions an XFe³⁺ value between 14% and 17% best represents the observations, similar to the analysis provided by Starr and Pattison (2019b); therefore, a ferric iron oxide value of 15% (equivalent to 8 mol% oxides) is used.

Modelling with data set ds5.5

Figures 9a and 9b show the equilibrium phase diagrams for the average low-Mg and the average high-Mg basalt bulk compositions in the NCKFMASHTO chemical system, calculated using the data set ds5.5 of Holland and Powell (1998). The calculated diagrams for the two bulk compositions show a number of similar features. In both sections, a large field containing the assemblage Act+Ab+Chl+Ep+Bt+Qtz+Ttn is present below 450 °C. Just upgrade of this field are two successive, relatively narrow fields (<20 °C wide) containing coexisting albite and oligoclase and coexisting hornblende and actinolite. The epidote-out reaction transects the fields of coexisting hornblende–actinolite–oligoclase and hornblende–oligoclase. The intersection between the actinolite-out and the epidote-out reactions occurs at 430 °C and 1.5 kbar for the low-Mg assemblage, and at 460 °C and 2.5 kbar for the high-Mg assemblage. Upgrade of the field of stability of hornblende–oligoclase, the chlorite-out reaction is predicted to occur at slightly lower temperatures in the low-Mg assemblage (525 °C), compared with the high-Mg assemblage (550 °C). Upgrade of the chlorite-out reaction, a relatively large field with the assemblage Hbl+Pl+Bt+Qtz+Ilm occurs. At relatively low pressures (<3.5 kbar) and high temperatures (>500 °C) magnetite is stable. Biotite is stable over the entire calculated P-T range.

Modelling with data set ds6.2

Figures 9c and 9d show the equilibrium phase diagrams for the average low-Mg and the average high-Mg basalt bulk composi-

Fig. 9. Pressure-temperature–equilibrium phase diagrams calculated in the NCKFMASHTO chemical system constructed for (a) the average low-Mg basalt in data set ds5.5; (b) the average high-Mg basalt in data set ds5.5; (c) the average low-Mg basalt in data set ds6.2; (d) the average high-Mg basalt in data set ds6.2. Fields are coloured according to mineral assemblage domains: green, Act+Ab+Chl; brown, Hbl+Act+Ab+Chl; orange, Hbl+Act+Pl+Chl; red, Hbl+Pl+Chl; purple, Hbl+Pl. (e) Modal volume of garnet in the MnNCKFMASHTO system for the average low-Mg basalt in data set ds5.5; (f) Mn in chlorite (cations per formula unit (cpfu)) in the MnNCKFMASHTO system for the average low-Mg basalt in data set ds5.5. Reaction lines for major mineral shown as solid lines; dotted lines used for accessory minerals. The dashed line intersecting the chlorite-out reaction is a modelling artefact, indicating the appearance of an additional amphibole. This amphibole is a theoretical phase calculated to handle structural order–disorder of Fe, Mg, and Al where the partitioning of these elements is unknown (camo1 and camo2; Diener and Powell 2012), and hence reflects the inability of the thermodynamic model to predict complex natural amphiboles in these bulk compositions. [Colour online.]

tions in the NCKFMASHTO chemical system, calculated using the data set ds6.2 of Holland and Powell (2011). Overall, the diagrams calculated with ds6.2 show the same fields as the models calculated with ds5.5, but in different positions. Compared with the diagrams calculated using ds5.5, the plagioclase-in and albite-out reactions occur at noticeably higher temperatures and are separated by a significant domain with the assemblage Hbl+Bt+Chl+Qtz+Ab+Pl ± Ttn ± Ilm that narrows with increasing pressure. The epidote-out reaction appears at the same position for calculations in ds5.5 and ds6.2, but the intersection with the actinolite-out isograd is observed at pressures <1.5 kbar using ds6.2. The chlorite-out reactions for both the low-Mg and high-Mg assemblage occur ~50 °C lower using ds6.2 compared with ds5.5. The reaction occurs at slightly lower temperatures in the low-Mg assemblage, compared with the high-Mg assemblage (480 °C in the low-Mg assemblage, 500 °C in the high-Mg assemblage). As in ds5.5, a large field with the assemblage Hbl+Pl+Bt+Qtz+Ilm is predicted upgrade of the chlorite-out reaction. These differences in the phase equilibria predicted using ds5.5 versus ds6.2 are very similar to those identified in Starr et al. (2020).

Comparison of observations from FF-AL sequence with predicted phase equilibria

In this section, the results of the thermodynamic modelling are compared with the natural observations from the FF-AL sequence. The aim is to assess the ability of the models to reproduce the natural mineral assemblages, and to assess whether discrepancies result from deficiencies in the thermodynamic modelling, or from departures from equilibrium conditions (cf. Starr and Pattison 2019a).

Differences between the observed mineral assemblages and predicted phase equilibria

Going through the greenschist–amphibolite transition, the observed sequence of isograds within the FF-AL sequence is Hbl-in, Olg-in, and Act-out. Hornblende and actinolite coexist between the Hbl-in and the Act-out isograds for up to 10 km, and upgrade of the Olg-in isograd, Ab and Olg coexist. Predicted phase equilibria using ds5.5 broadly reproduce the observed sequence of isograds between 3.7 and 4.2 kbar for the low-Mg basalt and 2.7–4.4 kbar for the high-Mg basalt, although not the spacing. For example, the significant observed width of domains in the field containing coexisting amphiboles, and coexisting plagioclase minerals, does not accord with the narrow predicted fields of coexisting amphiboles (Act/Hbl, <20 °C wide at >2.5 kbar) and feldspars (Ab/Olg, <5 °C wide). A possible explanation is the metastable persistence of these minerals to higher grade (Starr and Pattison 2019a). Predicted phase equilibria using ds6.2 only reproduces the observed sequence of isograds at very low pressures of <1.5 kbar for both bulk compositions. At more moderate pressures of 4–5 kbar, the appearance of oligoclase and disappearance of albite is predicted to occur at much higher temperatures (~100 °C higher) than the appearance of hornblende. As with the ds6.2 modelling, similar discrepancies occur in terms of the very small temperature intervals for coexisting amphiboles (Act/Hbl; <10 °C

wide field) and coexisting plagioclase (Ab/Olg; 50–100 °C wide field).

At higher grade, within the amphibolite facies, the natural sequence includes the disappearance of epidote, followed by the disappearance of chlorite and appearance of garnet. The Grt-in isograd is observed at the northern limit of the study area, down-grade of the transition into the KGB. Most rocks in the amphibolite facies contain titanite and ilmenite. Predicted phase equilibria using ds5.5 reproduce the observed sequence of isograds at <5 kbar and 475–500 °C for the low-Mg basalt and at <7 kbar and 475–500 °C for the high-Mg basalt. Discrepancies between nature and models include the prediction of coexisting titanite and ilmenite over a 10 °C range, and the calculation of the garnet-in reaction at anomalously high conditions of >680 °C and >8.8 kbar. For calculation with ds6.2, epidote disappears before chlorite at <3.5 kbar and 460 °C for the low-Mg assemblage, and at <7.5 kbar and 480 °C for the high-Mg assemblage. Other discrepancies, similar to those for ds5.5, are also observed, including <10 °C wide field for coexisting Fe–Ti oxides and the restriction of garnet to high pressures.

Assessment of thermodynamic databases

Previous studies of mineral assemblages within greenschist–amphibolite transitional sequences (Starr et al. 2020) have shown that low pressure, typically contact metamorphic, sequences are characterized by the appearance of oligoclase before hornblende, whereas in moderate pressure (Barrovian-type) sequences, hornblende appears before oligoclase. Based on these observations, it appears that models calculated with ds5.5 better represent the natural rocks. A central reason is that the sequence of hornblende-in, followed by oligoclase-in and actinolite-out, occurs at 2.7–4.4 kbar, which accords better with other data compared with <1.5 kbar predicted using ds6.2. Epidote-out followed by chlorite-out predicted at pressures up to 5 kbar using ds5.5 is also more realistic compared with a maximum predicted pressures of 3 and 1.75 kbar for the low-Mg and high-Mg bulk compositions, respectively, using ds6.2. The interval between oligoclase-in and albite-out appears to be better represented in models with ds6.2 (temperature range of 50–100 °C in ds6.2 compared with <5 °C in ds5.5), but for the high-Mg basalt this interval is only predicted at <2.5 kbar, which is interpreted to be too low pressure. This interpretation does not consider the possible metastable persistence of albite going upgrade, discussed below. Overall, the phase diagrams modelled using ds5.5 are able to better reproduce the observations from the FF-AL sequence. This observation is also in agreement with recent studies that have shown that ds6.2 poorly reproduces the stability of amphibole, garnet, and pyroxene (e.g., Forshaw et al. 2019; Santos et al. 2019; Starr et al. 2020).

Causes of discrepancies between model and nature

There are two possible major causes for the discrepancies between the natural sequence and calculated models. The first concerns possible deficiencies in the thermodynamic data set, in particular, the activity-composition models for individual minerals, resulting in difficulties simulating the behavior of the minerals in

the natural rocks. For example, the first appearance of garnet is predicted in ds5.5 in the NCKFMASHTO system at temperatures >680 °C and pressures >8.8 kbar. These conditions are too high compared with what has been observed in this study and reported by previous authors (Bailes and McRitchie 1978; Kraus and Menard 1997; Jungwirth et al. 2000). As Mn can also be an important control on the predicted stability of garnet (e.g., White et al. 2014), phase diagrams were also calculated in the system MnNCKFMASHTO for the low-Mg basaltic composition using the ds5.5 data set and a-X models (Figs. 9e, 9f). With Mn added to the system, garnet is predicted to be present over almost the entire P-T-section with modal amounts of up to 2.5% (Fig. 9e). For the set of ds5.5 a-X models used for the modelling in this study, Mn may be incorporated within garnet, chlorite, biotite, and ilmenite. While the predicted Mn contents of biotite and ilmenite are similar to those observed in the FF-AL sequence, the measured Mn in chlorite (up to 0.07 cpfu) is much higher compared with that predicted by the modelling (maximum of ~ 0.03 cpfu; Fig. 9f). The predicted stability of garnet at low P-T conditions suggests that the garnet model incorporates too much Mn, and (or) chlorite does not incorporate enough, which causes the overstabilization of garnet. In the case of the FF-AL sequence, garnet is only stable at higher grade across a discrete garnet-in isograd rather than being sporadically developed within rocks across a range of grades. Given that the rocks in the FF-AL sequence display variable Mn contents (0.10–0.30 wt% MnO), this observation suggests oversensitivity of the thermodynamic models to Mn content.

The second possible cause is that some minerals may not form part of the equilibrium assemblage. In particular, mineral-out reactions are complicated by possible metastable upgrade persistence of reactant minerals. For example, Starr and Pattison (2019a) have shown, in the Flin Flon area and elsewhere, that actinolite and hornblende coexist across a miscibility gap up to the oligoclase-in isograd, upgrade of which hornblende is the stable phase and actinolite persists as a metastable phase. Metastable persistence of actinolite means that the mapped actinolite-out isograd occurs at higher grade than predicted assuming equilibrium, implying an anomalously large interval of stable coexistence with hornblende. Similarly, albite is present in rocks quite far upgrade of the oligoclase-in isograd, in contrast to the predicted narrow interval of coexistence in the phase diagrams calculated using ds5.5.

Conditions of metamorphism

In this section, we use the thermodynamic modelling results, combined with observations from the FF-AL sequence, to estimate the P-T conditions for regional and contact metamorphism and the regional metamorphic field gradient.

Regional metamorphism

Two main constraints are used to determine the metamorphic field gradient for the FF-AL sequence: (1) the observed sequence of hornblende-in followed by oligoclase-in and actinolite-out, which is predicted to occur between 3.7 and 4.2 kbar at 450 °C for the low-Mg basalt and 2.7–4.4 kbar at 450 °C for the high-Mg basalt, using the modelling with ds5.5; and (2) the 1.5–2.3 kbar and 250–300 °C estimate of the P-T conditions estimated by Starr et al. (2020) for the prehnite–pumpellyite to greenschist facies transition using samples within the western portion of the field area, close to the townsite of Flin Flon. The resultant metamorphic field gradient of 100–150 °C/kbar is shown in Fig. 9a and 9b by the shaded area. Along the metamorphic field gradient, the predicted hornblende-in isograd occurs around 440–450 °C, followed by oligoclase-in at 450 °C, and actinolite-out at 450–460 °C. The epidote-out isograd is situated at approximately 475 °C, with the chlorite-out isograd predicted at 525 °C for the low-Mg assemblage and at 550 °C for the high-Mg assemblage.

Contact metamorphism

In the contact aureoles, the observed sequence of isograds in the low-Mg bulk composition with increasing grade is hornblende-in, oligoclase-in (and albite-out), biotite-in, and actinolite-out. A similar sequence lacking the biotite-in reaction is predicted for the high-Mg bulk composition (Fig. 9b). No epidote-out or chlorite-out isograds have been mapped within any of the contact aureoles. The garnet observed within contact metamorphic rocks is spatially limited to domains with different bulk compositions and so is not incorporated in the analysis. The observed sequence of hornblende-in followed by oligoclase-in (and albite-out) and actinolite-out is the same as the regional sequence, implying similar pressures of 3–4 kbar. As discussed in the regional metamorphic section, this sequence of mineral isograds is reproduced at conditions of 3.7–4.2 kbar and 450–470 °C for the low-Mg basalt, and 2.7–4.4 kbar and 430–470 °C for the high-Mg basalt (Figs. 9a, 9b). Comparing the modelled reaction with the observed isograds, in particular the lack of chlorite-out (and epidote-out) isograds, indicates peak metamorphic temperature of 450–500 °C. Temperatures close to the intrusions were probably higher than this, but were not determined, likely a function of the limited sampling resolution.

Geothermal gradient

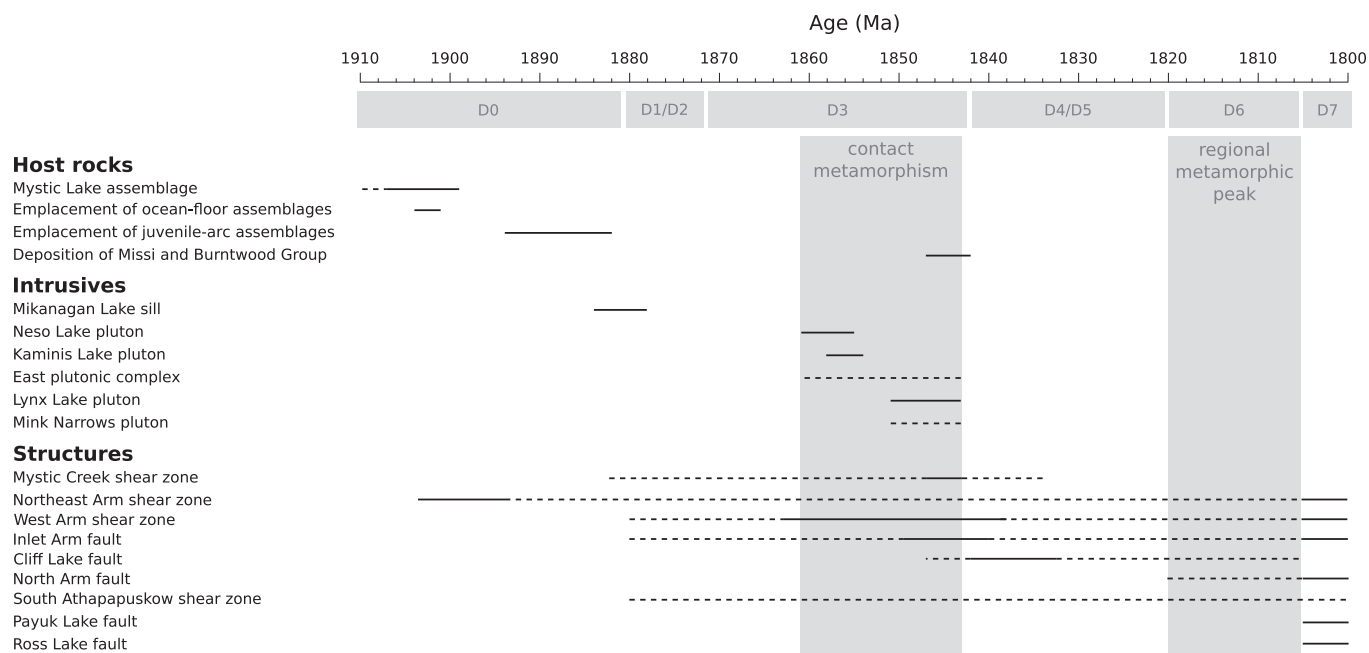
A range of geothermal gradients at the time of metamorphism for the Athapuskow Lake area is approximated using the P-T constraints for the prehnite–pumpellyite–greenschist and greenschist–amphibolite facies transitions listed above, and assuming an average density of mafic rocks of 2800–3000 kg/m³. For the island-arc assemblages (low-Mg basalts) the values range between 25 and 31 °C/km, whereas for the ocean-floor assemblages (high-Mg basalts) the values range between 26 and 50 °C/km. Bailes (1979) reported a similar geothermal gradient of 35–45 °C/km for the transition from the FFB to the KGB in the File Lake area. These estimates are similar to estimates proposed for Proterozoic continental crust (25–35 °C/km; Lambert 1983), but differ considerably from the average for modern continental crust (17 °C/km; Burke and Kidd 1978). The steep geothermal gradient determined from the mafic rocks of the FF-AL sequence extends across the KGB. This observation is consistent with previous studies that argued that the metamorphic transition from the FFB into the KGB is continuous (e.g., Bailes 1980; this study) and only locally interrupted by faults (Zwanzig and Bailes 2010; Gilbert 2012). There is no evidence of post-metamorphic deformation along structures important enough to affect the metamorphic field gradient (and the geothermal gradient).

The steep geothermal gradient is possibly due to the fact that relatively thin oceanic crustal domains were juxtaposed prior to accretion with the continental margin, generating a higher geothermal gradient compared with typical continental crust. It is also possible that the steep geothermal gradient reflects higher heat flow in the KGB compared with the FFB, in which case increased heat flow could be due to some combination of (1) higher heat flow from decay of radiogenic elements due to more potassic composition of the metasediments of the KGB compared with the metavolcanics of the FFB (e.g., Huerta et al. 1998), (2) higher heat flow from hot material rising under the KGB through intrusions of sills or mantle exhumation through crustal delamination (e.g., Menard and Gordon 1997), and (3) higher thermal conductivity of sediments compared with volcanic rocks (e.g., Clauser and Huenges 1995).

Geologic evolution of the FF-AL

The new metamorphic and structural relationships in the FF-AL presented in this paper refine the tectono-metamorphic models for the west-central FFB proposed by previous authors (e.g., Lucas et al. 1996; Syme 2015; Lafrance et al. 2016). The following section

Fig. 10. Overview of magmatic, structural, and metamorphic events in the Flin Flon – Athapapuskow Lake area. Deformation events D0–D7 from Lafrance et al. (2016), see text for references. Dashed lines, probable time range; solid lines, defined time range.



and Fig. 10 summarize the evolution of the FF-AL incorporating new insights obtained from this study.

The MLA is one of the oldest domains in the FF-AL (>1903 +6/−4 Ma; Stern et al. 1993), emplaced after the ocean floor assemblages at 1904–1901 Ma (Syme 2015) and before the arc assemblages at 1894–1882 Ma (Syme 2015). Based on geochemical and geochronological evidence, Lucas et al. (1996) interpreted the MLA to represent a tectonic slice of the middle crust of an arc built on Archean crust, possibly a fragment of a microcontinent. We suggest that the heat of the felsic intrusions (1903 +6/−4 Ma; Stern et al. 1993) within the MLA may have contributed to the amphibolite-facies metamorphism of the mafic host rocks, pre-dating the main phase of regional metamorphism. This is in part evidenced by the distinct difference in metamorphic grade between the amphibolite facies MLA and the surrounding regionally metamorphosed rocks of prehnite–pumpellyite grade. The evidence for protracted displacement and deformation along the Namew Lake structure (Fig. 1) may have resulted in the MLA's strong foliation.

The FF-AL mainly consists of arc and ocean-floor assemblage volcanic, and related intrusive and sedimentary rocks. Ocean-floor assemblages (1904–1901 Ma; Syme 2015) are separated from slightly younger arc assemblages (1894–1882 Ma; Syme 2015) by the Mistik Creek shear zone (e.g., Lucas et al. 1996; Syme 2015), suggesting that the Mistik Creek shear zone is one of the earliest active structures in the FF-AL. Displacement of metamorphic isograds suggests that the shear zone was reactivated at least once after the regional metamorphic peak.

Successor-arc intrusions occur within the arc assemblage shortly after this was emplaced between 1884 and 1843 Ma. The Mikanagan sill and related magmatic bodies intrude the arc assemblage at 1881 ± 3 Ma (Stern et al. 1999). Between 1861 and 1843 Ma, the Neso Lake pluton, the Kaminis Lake pluton, the East plutonic complex, and the Lynx Lake pluton were emplaced (Syme et al. 1991; Stern and Lucas 1994; Stern et al. 1999). Mineral assemblages in the contact aureoles, combined with thermodynamic modelling, suggest that the pressure of emplacement of the intrusions in the southern part of the field area where the aureoles can be recognized was between 2.7 and 4.4 kbar.

The presence of deformed volcanic sediments within the West Arm shear zone (Stern et al. 1999) and the interpretation that the Phantom Lake pluton cuts the West Arm shear zone (Heaman et al. 1992), suggests that the structure was active between 1863 and 1838 Ma. However, the results of our study show that greenschist and amphibolite facies assemblages are juxtaposed against prehnite–pumpellyite facies assemblages across the shear zone, indicating that the structure must have been re-activated after the metamorphic peak at 1820–1805 Ma.

Between the emplacement of the intrusions (1861–1843 Ma; Gordon et al. 1990; Syme et al. 1991; Stern et al. 1999; Stern and Lucas 1994; Whalen et al. 2016) and the deposition of the continentally derived Missi Group sediments (1847–1842 Ma; Ansdell et al. 1995; Lucas et al. 1996), the Inlet Arm fault was active. Displacement of isograds across the fault, however, indicates that this structure, even if initiated relatively early, also experienced re-activation following the metamorphic peak. All the structures active prior to the deposition of the sediments are characterized by ductile fabrics. They commonly juxtapose different lithostratigraphic units and are interpreted to be associated with accretion of the island-arc and ocean-floor assemblages.

The Payuk Lake fault deforms the Lynx Lake pluton (1847 Ma; Gordon et al. 1990) suggesting it was active after the emplacement of the intrusion. The Cliff Lake fault displaces the Missi Group sedimentary rocks around the town of Flin Flon (1842 Ma; Lafrance et al. 2016), which indicates it was active after the deposition of the sediments.

All deformed rocks within faults or shear zones are metamorphosed (greenschist facies assemblages). The metamorphic grade of rocks within the structures does not always correspond to the grade of the surrounding units (for example, greenschist facies assemblages in rocks of the North Arm fault are surrounded by prehnite–pumpellyite facies units), suggesting a role for frictional heating and (or) advected hot fluids along major faults.

The regional metamorphic peak was reached around 1820–1805 Ma in the eastern part of the FFB (e.g., Gordon et al. 1990; Ansdell and Norman 1995; David et al. 1996) and affects the majority of the rock units. Several of the early structures show evidence of post-metamorphic re-activation based on displacement

of metamorphic isograds and difference in metamorphic grade within the structure compared with the surrounding host rocks. The late movements are interpreted to be associated with continued collision between the Flin Flon – Glennie Complex and the Sask and Superior cratons after peak metamorphism. Evidence for activation of a number of shear zone and faults before and after peak metamorphism shows that the FF-AL experienced multiple deformational events occurring over a prolonged period of time. Similar behavior has been reported in a number of accretionary orogens (e.g., [Cawood et al. 2009](#)).

The last faults to develop — the Ross Lake fault, North Arm fault, and the South Athapapuskow shear zone — cut earlier structures, exhibit brittle–ductile features, and displace metamorphic isograds, and thus were active after the regional metamorphic peak. Movement along these structures is interpreted to be related to post-collisional tectonism, and possibly tectonic relaxation.

Conclusions

The FF-AL is characterized by an amalgamation of metamorphosed volcanic, intrusive, and sedimentary rocks juxtaposed by a series of shear zones and faults. The metamorphic grade increases from south to north from prehnite–pumpellyite to amphibolite facies. New petrographic data and increased sampling resolution have resulted in a more detailed metamorphic map of mineral assemblage zones and isograds in the widespread metabasic rocks in the area. This has permitted a better understanding of the relationships amongst intrusions, shear zone development, and metamorphism. The main conclusions of the study are as follows:

1. Ten regional metamorphic zones separated by nine isograds were identified. From south to north (with increasing grade), the isograds are prehnite- and pumpellyite-out, actinolite-in, biotite-in, hornblende-in, oligoclase-in, actinolite-out, epidote-out, chlorite-out, and garnet-in. The low grade part comprises the same sequence of metamorphic zones and isograds as reported by [Starr and Pattison \(2019a, 2019b\)](#) and [Starr et al. \(2020\)](#) for the Flin Flon area.
2. A comparison between observed and modelled reactions was carried out to evaluate the ability of the models to reproduce the natural sequence of mineral assemblages and test the validity of P-T estimates. Models were calculated for the internally consistent databases of [Holland and Powell \(1998; ds5.5\)](#) and [Holland and Powell \(2011, ds6.2\)](#). Models calculated with data set ds5.5 in the NCKFMASHTO chemical system, with an $X_{Fe^{3+}}$ content of 15%, predict the same sequence of isograds as observed in the natural sequence at realistic pressure conditions (3–6 kbar). Models calculated with data set ds6.2 only partially reproduce the observed sequence and only at pressures that are interpreted to be too low (<1.5 kbar).
3. Although providing a good general quantification of the metamorphic conditions, several discrepancies between natural and modelled sequences exist, including the absence of an albite-out isograd in the field; the wide observed zones of co-existence of actinolite and hornblende, and albite and oligoclase, that are not reproduced in the models; and the high sensitivity in the modelled phase equilibria to Mn content that is not indicated within the FF-AL metabasites. These discrepancies are mainly due to limitations in the thermodynamic a-X models for some of the complex minerals involved in the metamorphic sequence, and metastable persistence of some minerals to higher grade due to sluggish reaction kinetics.
4. The thermodynamic modelling suggests that the metamorphosed mafic rocks in the southern part of the FF-AL reached about 430–480 °C and 3–4.5 kbar at the greenschist–amphibolite facies transition. Contact aureoles recognized in the southern part of the FF-AL that predated regional metamorphism attained temperatures of 500 °C close to the respective intrusions at a pressure between 2.7 and 4.4 kbar, about the same pressures as the regional metamorphism.
5. A metamorphic field gradient of 100–150 °C/kbar was approximated by comparing the 250–300 °C and 1.5–2.3 kbar conditions estimated for the prehnite–pumpellyite to greenschist facies transition, and the 430–480 °C and 3–4.5 kbar conditions estimated for the greenschist to amphibolite facies transition.
6. The metamorphic field gradient was used to estimate a range of geothermal gradients for the FF-AL. Combining the values calculated for the island-arc (low-Mg) and ocean-floor (high-Mg) assemblages, an approximate geothermal gradient between 25 and 31 °C/km is estimated for the FF-AL area. A steep geothermal gradient extends across the FFB and the KGB.

This increase in heat flow could be the result of the accretion of oceanic crust onto the continental margin or could be caused by higher heat flow generated by the decay of radiogenic elements of rocks with potassic bulk compositions, higher heat flow from rising magma under the KGB, and higher thermal conductivity of sediments compared with volcanic rocks.

Acknowledgements

This project would not have been possible without the support of the Manitoba Geological Survey, which provided field logistics and access to archived rock samples and thin sections. We thank R. Marr at the University of Calgary for help with operating the electron microprobe. We also thank K. Ansdell and C. Yakymchuk for providing insightful reviews and the handling editor, T. Rivers, for detailed comments that greatly improved this paper. This research was partially supported by Natural Sciences and Engineering Research Council of Canada (NSERC) Discovery Grant 037233 to D.R.M. Pattison.

References

- Ansdell, K.M. 2005. Tectonic evolution of the Manitoba-Saskatchewan segment of the Paleoproterozoic Trans-Hudson Orogen, Canada. *Canadian Journal of Earth Sciences*, **42**(4): 741–759. doi:10.1139/e05-035.
- Ansdell, K.M., and Norman, A.R. 1995. U Pb geochronology and tectonic development of the southern flank of the Kiseynew Domain. *Precambrian Research*, **72**: 147–167. doi:10.1016/0301-9268(94)00090-E.
- Ansdell, K.M., Lucas, S.B., Connors, K., and Stern, R.A. 1995. Kiseynew metasedimentary gneiss belt, Trans-Hudson orogen (Canada): back-arc origin and collisional inversion. *Geology*, **23**: 1039–1043. doi:10.1130/0091-7613(1995)023<1039:KMGTH>2.3.CO;2.
- Ashton, K. 1993. Structure of the southern flank of the Kiseynew Gneiss Belt in Saskatchewan. *Trans-Hudson Orogen Transect, Report of Third Transect Meeting*, Regina, Saskatchewan, pp. 84–87.
- Ashton, K., Lewry, J., Heaman, L., Hartlaub, R., Stauffer, M., and Tran, H. 2005. The Pelican Thrust Zone: basal detachment between the Archean Sask Craton and Paleoproterozoic Flin Flon Glennie Complex, western Trans-Hudson Orogen. *Canadian Journal of Earth Sciences*, **42**(4): 685–706. doi:10.1139/e04-035.
- Ashworth, J.R., and Evirgen, M.M. 1985. Plagioclase relations in pelites, central Menderes Massif, Turkey. I. The peristerite gap with coexisting kyanite. *Journal of Metamorphic Geology*, **3**(3): 207–218. doi:10.1111/j.1525-1314.1985.tb00317.x.
- Bailes, A. 1979. Sedimentology and metamorphism of a Proterozoic volcanoclastic turbidite suite that crosses the boundary between the Flin Flon and Kiseynew belts. File Lake, Manitoba, Canada, University of Manitoba.
- Bailes, A. 1980. Geology of the File Lake area Manitoba Department of Energy and Mines. Mineral Resource Division, Manitoba Department of Energy and Mines, Manitoba.
- Bailes, A., and McRitchie, W. 1978. The transition from low to high grade metamorphism in the Kiseynew sedimentary gneiss belt, Manitoba. *In* *Metamorphism in the Canadian Shield*. Geological Survey of Canada Paper 78-10.
- Bailes, A., and Syme, E. 1989. Geology of the Flin Flon–White Lake area. Manitoba Energy and Mines, Winnipeg, Man. Geological report (Manitoba. Geological Services Branch), GR 87-1.
- Bickford, M., Collerson, K., Lewry, J., Van Schmus, W., and Chiarenzelli, J. 1990. Proterozoic collisional tectonism in the Trans-Hudson orogen, Saskatchewan. *Geology*, **18**: 14–18. doi:10.1130/0091-7613(1990)018<0014:PCITTT>2.3.CO;2.
- Bleeker, W. 1990. New structural-metamorphic constraints on Early Proterozoic oblique collision along the Thompson Nickel Belt, Manitoba, Canada. *In* *The early Proterozoic Trans-Hudson orogen of North America*. Edited by J.F. Lewry

- and M.R. Stauffer. Geological Association of Canada, Special Paper 37, pp. 57–73.
- Burke, K., and Kidd, W. 1978. Were Archean continental geothermal gradients much steeper than those of today? *Nature*, **272**: 240–241. doi:10.1038/272240a0.
- Carpenter, M.A. 1981. A “conditional spinodal” within the peristerite miscibility gap of plagioclase feldspars. *American Mineralogist*, **66**(5–6): 553–560.
- Cawood, P.A., Kröner, A., Collins, W.J., Kusky, T.M., Mooney, W.D., and Windley, B.F. 2009. Accretionary orogens through Earth history. Geological Society, London, Special Publications, **318**: 1–36. doi:10.1144/SP318.1.
- Clauser, C., and Huenges, E. 1995. Thermal conductivity of rocks and minerals. In *Rock physics and phase relations: a handbook of physical constants*. American Geophysical Union (part of the AGU Reference Shelf Series). Vol. 3, pp. 105–126.
- Coggon, R., and Holland, T. 2002. Mixing properties of phengitic micas and revised garnet-phengite thermobarometers. *Journal of Metamorphic Geology*, **20**: 683–696. doi:10.1046/j.1525-1314.2002.00395.x.
- David, J., Bailes, A., and Machado, N. 1996. Evolution of the Snow Lake portion of the Palaeoproterozoic Flin Flon and Kiseynew belts, Trans-Hudson Orogen, Manitoba, Canada. *Precambrian Research*, **80**: 107–124. doi:10.1016/S0303-9268(96)00008-3.
- de Capitani, C., and Brown, T.H. 1987. The computation of chemical equilibrium in complex systems containing non-ideal solutions. *Geochimica et Cosmochimica Acta*, **51**: 2639–2652. doi:10.1016/0016-7037(87)90145-1.
- de Capitani, C., and Petrakakis, K. 2010. The computation of equilibrium assemblage diagrams with Theriak/Domino software. *American Mineralogist*, **95**: 1006–1016. doi:10.2138/am.2010.3354.
- Diener, J., and Powell, R. 2012. Revised activity-composition models for clinopyroxene and amphibole. *Journal of Metamorphic Geology*, **30**: 131–142. doi:10.1111/j.1525-1314.2011.00959.x.
- Digel, S., and Ghent, E. 1994. Fluid-mineral equilibria in prehnite-pumpellyite to greenschist facies metabasites near Flin Flon, Manitoba, Canada: implications for petrogenetic grids. *Journal of Metamorphic Geology*, **12**: 467–477. doi:10.1111/j.1525-1314.1994.tb00036.x.
- Digel, S., and Gordon, T. 1993. Quantitative estimates of pressure–temperature–fluid composition in metabasites from prehnite-pumpellyite to amphibolite facies near Flin Flon. *Trans-Hudson Orogen Transect. Lithoprobe Report*, pp. 139–156.
- Ellis, S., Beaumont, C., and Pfiffner, O.A. 1999. Geodynamic models of crustal-scale episodic tectonic accretion and underplating in subduction zones. *Journal of Geophysical Research: solid Earth*, **104**: 15169–15190. doi:10.1029/1999JB900071.
- Fedorowich, J., Kerrich, R., and Stauffer, M. 1995. Geodynamic evolution and thermal history of the central Flin Flon Domain, Trans-Hudson Orogen: constraints from structural development, $^{40}\text{Ar}/^{39}\text{Ar}$, and stable isotope geothermometry. *Tectonics*, **14**: 472–503. doi:10.1029/94TC01318.
- Forshaw, J.B., Waters, D.J., Pattison, D.R., Palin, R.M., and Gopon, P. 2019. A comparison of observed and thermodynamically predicted phase equilibria and mineral compositions in mafic granulites. *Journal of Metamorphic Geology*, **37**(2): 153–179. doi:10.1111/jmg.12454.
- Gale, D., Lucas, S., and Dixon, J. 1999. Structural relations between the polydeformed Flin Flon arc assemblage and Missi Group sedimentary rocks, Flin Flon area, Manitoba and Saskatchewan. *Canadian Journal of Earth Sciences*, **36**(11): 1901–1915. doi:10.1139/e99-099.
- Gilbert, H.P. 2012. Geology and geochemistry of arc and ocean-floor volcanic rocks in the northern Flin Flon Belt, Embury–Wabishkok–Naosap lakes area, Manitoba (parts of NTS 63K13, 14). Manitoba Innovation, Energy and Mines, Manitoba Geological Survey, Geoscientific Report GR2011-1, 46pp.
- Gordon, T., Hunt, P., Bailes, A., and Syme, E. 1990. U-Pb ages from the Flin Flon and Kiseynew belts, Manitoba: chronology of crust formation at an Early Proterozoic accretionary margin. The Early Proterozoic Trans-Hudson Orogen of North America. Edited by J.F. Lewry and M.R. Stauffer. Geological Association of Canada, Special Paper 37, pp. 177–199.
- Green, E., White, R., Diener, J., Powell, R., Holland, T., and Palin, R. 2016. Activity-composition relations for the calculation of partial melting equilibria in metabasic rocks. *Journal of Metamorphic Geology*, **34**: 845–869. doi:10.1111/jmg.12211.
- Heaman, L.M., Kamo, S.L., Ashton, K.E., Reilly, B.A., Slimmon, W.L., and Thomas, D.J. 1992. U-Pb geochronological investigations in the Trans-Hudson Orogen, Saskatchewan. Summary of Investigations, 1992, Saskatchewan Geological Survey, Saskatchewan Energy Mines, Miscellaneous Report, 92-4, pp. 120–123.
- Hey, M.H. 1954. A new review of the chlorites. *Mineralogical Magazine and Journal of the Mineralogical Society*, **30**: 277–292. doi:10.1180/minmag.1954.030.224.01.
- Heywood, W.W. 1966. Ledge Lake Area, Manitoba and Saskatchewan. Department of Mines and Technical Surveys, Canada.
- Hoffman, P.F. 1988. United Plates of America, the birth of a craton-early Proterozoic assembly and growth of Laurentia. *Annual Review of Earth and Planetary Sciences*, **16**: 543–603. doi:10.1146/annurev.earth.16.050188.002551.
- Holland, T., and Powell, R. 1998. An internally consistent thermodynamic data set for phases of petrological interest. *Journal of Metamorphic Geology*, **16**: 309–343. doi:10.1111/j.1525-1314.1998.00140.x.
- Holland, T., and Powell, R. 2003. Activity-composition relations for phases in petrological calculations: an asymmetric multicomponent formulation. *Contributions to Mineralogy and Petrology*, **145**: 492–501. doi:10.1007/s00410-003-0464-z.
- Holland, T., and Powell, R. 2011. An improved and extended internally consistent thermodynamic dataset for phases of petrological interest, involving a new equation of state for solids. *Journal of Metamorphic Geology*, **29**: 333–383. doi:10.1111/j.1525-1314.2010.00923.x.
- Huerta, A.D., Royden, L.H., and Hodges, K.V. 1998. The thermal structure of collisional orogens as a response to accretion, erosion, and radiogenic heating. *Journal of Geophysical Research: solid Earth*, **103**: 15287–15302. doi:10.1029/98JB00593.
- Jungwirth, T., Gordon, T.M., and Froese, E. 2000. Metamorphism of the Burntwood Group in the Duval Lake area, Manitoba, Canada. *The Canadian Mineralogist*, **38**: 435–442. doi:10.2113/gscanmin.38.2.435.
- Kraus, J., and Menard, T. 1997. A thermal gradient at constant pressure; implications for low-to medium-pressure metamorphism in a compressional tectonic setting, Flin Flon and Kiseynew domains, Trans-Hudson Orogen, central Canada. *The Canadian Mineralogist*, **35**: 1117–1136.
- Lafrance, B., Gibson, H., Pehrsson, S., Schetselaar, E., DeWolfe, M., and Lewis, D. 2016. Structural reconstruction of the Flin Flon volcanogenic massive sulfide mining district, Saskatchewan and Manitoba, Canada. *Economic Geology*, **111**(4): 849–875. doi:10.2113/econgeo.111.4.849.
- Lambert, R.S.J. 1983. Metamorphism and thermal gradients. In *Proterozoic continental crust Proterozoic geology: selected papers from an International Proterozoic Symposium*, Vol. 161, pp. 155–156.
- Leake, B.E., Woolley, A.R., Arps, C.E., Birch, W.D., Gilbert, M.C., Grice, J.D., et al. 1997. Nomenclature of amphiboles; report of the Subcommittee on Amphiboles of the International Mineralogical Association Commission on new minerals and mineral names. *Mineralogical Magazine*, **61**: 295–310. doi:10.1180/minmag.1997.061.405.13.
- Lucas, S., Stern, R., Syme, E., Reilly, B., and Thomas, D. 1996. Intraoceanic tectonics and the development of continental crust: 1.92–1.84 Ga evolution of the Flin Flon Belt, Canada. *Geological Society of America Bulletin*, **108**: 602–629. doi:10.1130/0016-7606(1996)108<0602:ITATDO>2.3.CO;2.
- Maruyama, S., Liou, J.G., and Suzuki, K. 1982. The peristerite gap in low-grade metamorphic rocks. *Contributions to Mineralogy and Petrology*, **81**(4): 268–276. doi:10.1007/BF00371681.
- Menard, T., and Gordon, T.M. 1997. Metamorphic P-T paths from the eastern Flin Flon Belt and Kiseynew Domain, Snow Lake, Manitoba. *The Canadian Mineralogist*, **35**: 1093–1116.
- Moore, J., and Froese, E. 1972. Geological setting of the Snow Lake area Report of Activities. Geological Survey of Canada Paper, pp. 78–81.
- Santos, C.A., Moraes, R., and Szabó, G.A. 2019. A comparison between phase diagram modelling of metamafic rocks and experimental and independent thermobarometric data. *Lithos*, **340**: 108–123. doi:10.1016/j.lithos.2019.04.024.
- Schneider, D., Heizler, M., Bickford, M., Wortman, G., Condie, K., and Perilli, S. 2007. Timing constraints of orogeny to cratonization: thermochronology of the Paleoproterozoic Trans-Hudson orogen, Manitoba and Saskatchewan, Canada. *Precambrian Research*, **153**: 65–95. doi:10.1016/j.precamres.2006.11.007.
- Schumacher, J.C. 1997. Appendix 2: the estimation of ferric iron in electron microprobe analysis of amphiboles. *Mineralogical Magazine*, **61**: 312–321. doi:10.1017/S0026461X00011397.
- Starr, P.G. 2017. Sub-greenschist to lower amphibolite facies metamorphism of basalts: examples from Flin Flon, Manitoba and Rossland, British Columbia. Ph.D. thesis, University of Calgary, Calgary, Alta.
- Starr, P.G., and Pattison, D.R. 2019a. Equilibrium and disequilibrium processes across the greenschist–amphibolite transition zone in metabasites. *Contributions to Mineralogy and Petrology*, **174**: 18. doi:10.1007/s00410-019-1553-y.
- Starr, P.G., and Pattison, D.R. 2019b. Metamorphic devolatilization of basalts across the greenschist–amphibolite facies transition zone: insights from isograd mapping, petrography and thermodynamic modelling. *Lithos*, **342**: 295–314. doi:10.1016/j.lithos.2019.05.020.
- Starr, P.G., Pattison, D.R., and Ames, D.E. 2020. Mineral assemblages and phase equilibria of metabasites from the prehnite–pumpellyite to amphibolite facies, with the Flin Flon Greenstone Belt (Manitoba) as a type example. *Journal of Metamorphic Geology*, **38**(1): 71–102. doi:10.1111/jmg.12513.
- Stern, R., and Lucas, S. 1994. U-Pb zircon age constraints on the early tectonic history of the Flin Flon accretionary collage, Saskatchewan. *Geological Survey of Canada Current Research 1994-F*, pp. 75–86. doi:10.4095/195173.
- Stern, R.A., Syme, E.C., and Lucas, S.B. 1995a. Geochemistry of 1.9 Ga MORB- and OIB-like basalts from the Amisk collage, Flin Flon Belt, Canada: evidence for an intra-oceanic origin. *Geochimica et Cosmochimica Acta*, **59**: 3131–3154. doi:10.1016/0016-7037(95)00202-B.
- Stern, R.A., Lucas, S.B., Syme, E.C., Bailes, A.H., Thomas, D.J., Leclair, A.D., and Hulbert, L. 1993. Geochronological studies in the NATMAP Shield Margin Project area, Flin Flon domain: results for 1992–1993, in *Radiogenic Age and Isotopic Studies: report 7*. Geological Survey of Canada, Paper 93-2, pp. 59–70.
- Stern, R.A., Syme, E.C., Bailes, A.H., and Lucas, S.B. 1995b. Paleoproterozoic (1.90–1.86 Ga) arc volcanism in the Flin Flon Belt, Trans-Hudson Orogen,

- Canada. Contributions to Mineralogy and Petrology, **119**: 117–141. doi:10.1007/BF00307276.
- Stern, R., Machado, N., Syme, E., Lucas, S., and David, J. 1999. Chronology of crustal growth and recycling in the Paleoproterozoic Amisk collage (Flin Flon Belt), Trans-Hudson orogen, Canada. Canadian Journal of Earth Sciences, **36**(11): 1807–1827. doi:10.1139/e99-028.
- Stockwell, C. 1946. Flin Flon-Mandy Area, Manitoba and Saskatchewan. Geological Survey of Canada.
- Syme, E.C. 2015. Geology of the Athapapuskow Lake area, western Flin Flon belt, Manitoba (part of NTS 63K12), Manitoba Mineral Resources, Manitoba Geological Survey, Geoscientific Report GR2014-1.
- Syme, E., and Bailes, A. 1993. Stratigraphic and tectonic setting of early Proterozoic volcanogenic massive sulfide deposits, Flin Flon, Manitoba. Economic Geology, **88**: 566–589. doi:10.2113/gsecongeo.88.3.566.
- Syme, E.C., Hunt, P.A., and Gordon, T.M. 1991. Two U-Pb zircon ages from the western Flin Flon belt, Trans-Hudson orogen, Manitoba, in Radiogenic age and isotopic studies: report 4, Geol. Surv. Can., Pap. 90-2, pp. 25–34.
- Syme, E., Lucas, S., Zwanzig, H., Bailes, A., Ashton, K., and Haidl, F. 1998. Geology, NATMAP Shield Margin Project area, Flin Flon Belt, Manitoba/Saskatchewan, MAP 1998A Geological Survey of Canada, MAP.
- Syme, E., Lucas, S., Bailes, A., and Stern, R. 1999. Contrasting arc and MORB-like assemblages in the Paleoproterozoic Flin Flon Belt, Manitoba, and the role of intra-arc extension in localizing volcanic-hosted massive sulphide deposits. Canadian Journal of Earth Sciences, **36**: 1767–1788. doi:10.1139/e98-084.
- Thomas, D.J. 1991. Revision bedrock geological mapping: bootleg Lake-Birch Lake area (parts of NTS 63K-12 and 63L-9). In Summary of Investigations, Saskatchewan Geological Survey, Saskatchewan Energy and Mines, Miscellaneous Report 91-4, pp. 2–8.
- Whalen, J.J., Pehrsson, S.J., and Rayner, N.M. 2016. Significance of pre-1860 Ma granitoid magmatism for crustal evolution and exploration targeting in the Flin Flon assemblage, Trans-Hudson orogen, Canada. Economic Geology, **111**: 1021–1039. doi:10.2113/econgeo.111.4.1021.
- Whalen, J.B., Syme, E.C., and Stern, R.A. 1999. Geochemical and Nd isotopic evolution of Paleoproterozoic arc-type granitoid magmatism in the Flin Flon Belt, Trans-Hudson orogen, Canada. Canadian Journal of Earth Sciences, **36**(2): 227–250. doi:10.1139/e98-026.
- White, R., Powell, R., and Holland, T. 2007. Progress relating to calculation of partial melting equilibria for metapelites. Journal of Metamorphic Geology, **25**: 511–527. doi:10.1111/j.1525-1314.2007.00711.x.
- White, R.W., Powell, R., Holland, T.J.B., and Worley, B.A. 2000. The effect of TiO₂ and Fe₂O₃ on metapelitic assemblages at greenschist and amphibolite facies conditions: mineral equilibria calculations in the system K₂O-FeO-MgO-Al₂O₃-SiO₂-H₂O-TiO₂-Fe₂O₃. Journal of Metamorphic Geology, **18**(5): 497–512. doi:10.1046/j.1525-1314.2000.00269.x.
- White, R.W., Powell, R., and Clarke, G.L. 2002. The interpretation of reaction textures in Fe-rich metapelitic granulites of the Musgrave Block, central Australia: constraints from mineral equilibria calculations in the system K₂O-FeO-MgO-Al₂O₃-SiO₂-H₂O-TiO₂-Fe₂O₃. Journal of Metamorphic Geology, **20**(1): 41–55. doi:10.1046/j.0263-4929.2001.00349.x.
- White, R., Powell, R., Holland, T., Johnson, T., and Green, E. 2014. New mineral activity-composition relations for thermodynamic calculations in metapelitic systems. Journal of Metamorphic Geology, **32**: 261–286. doi:10.1111/jmg.12071.
- Whitney, D.L., and Evans, B.W. 2010. Abbreviations for names of rock-forming minerals. American Mineralogist, **95**: 185–187. doi:10.2138/am.2010.3371.
- Zwanzig, H.V., and Bailes, A.H. 2010. Geology and geochemical evolution of the northern Flin Flon and southern Kisseynew domains, Kisseynew-File lakes area, Manitoba (parts of NTS 63K, N). Innovation, Energy and Mines, Manitoba Geological Survey, 135.pp